

Stochastic Coverage in Heterogeneous Sensor Networks

LOUKAS LAZOS and RADHA POOVENDRAN
Network Security Lab, University of Washington

We study the problem of *coverage* in planar heterogeneous sensor networks. Coverage is a performance metric that quantifies how well a field of interest is monitored by the sensor deployment. To derive analytical expressions of coverage for heterogeneous sensor networks, we formulate the coverage problem as a set intersection problem, a problem studied in integral geometry. Compared to previous analytical results, our formulation allows us to consider a network model where sensors are deployed according to an arbitrary stochastic distribution; sensing areas of sensors need not follow the unit disk model but can have any arbitrary shape; sensors need not have an identical sensing capability. Furthermore, our formulation does not assume deployment of sensors over an infinite plane and, hence, our derivations do not suffer from the border effect problem arising in a bounded field of interest. We compare our theoretical results with the spatial Poisson approximation that is widely used in modeling coverage. By computing the Kullback-Leibler and total variation distance between the probability density functions derived via our theoretical results, the Poisson approximation, and the simulation, we show that our formulas provide a more accurate representation of the coverage in sensor networks. Finally, we provide examples of calculating network parameters such as the network size and sensing range in order to achieve a desired degree of coverage.

Categories and Subject Descriptors: C.2 [**Computer-Communication Networks**]; C.2.1 [**Computer-Communication Networks**]: Network Architecture and Design—*Distributed networks; network topology*

General Terms: Algorithm, Design, Performance

Additional Key Words and Phrases: Stochastic, coverage, sensor networks, heterogeneous

1. INTRODUCTION

Sensor networks are becoming an attractive solution for many commercial and military applications due to their low cost, ease of deployment, unattended operation, and wealth of useful information that they can collect. Typical applications include emergency rescue, ambient control, environmental monitoring,

This work was supported in part by the following grants: ONR YIP award, N00014-04-1-0479, ARO PECASE grant, W911NF-05-1-0491.

Authors' address: Department of Electrical Engineering, University of Washington, Paul Allen Center—Room AE100R, Campus Box 352500, Seattle, WA 98195-2500; email: {llazos, rp3}@u.washington.edu.

Permission to make digital or hard copies of part or all of this work for personal or classroom use is granted without fee provided that copies are not made or distributed for profit or direct commercial advantage and that copies show this notice on the first page or initial screen of a display along with the full citation. Copyrights for components of this work owned by others than ACM must be honored. Abstracting with credit is permitted. To copy otherwise, to republish, to post on servers, to redistribute to lists, or to use any component of this work in other works requires prior specific permission and/or a fee. Permissions may be requested from Publications Dept., ACM, Inc., 2 Penn Plaza, Suite 701, New York, NY 10121-0701 USA, fax +1 (212) 869-0481, or permissions@acm.org.
© 2006 ACM 1550-4859/06/0800-0325 \$5.00

home health care, and surveillance networks [Akyildiz et al. 2002; Mainwaring et al. 2002].

One of the primary tasks of sensor networks is to monitor a field of interest (*FoI*). Sensors may monitor physical properties such as temperature, humidity, and air quality, or track the motion of objects moving within the *FoI*. In many cases sensor networks may initiate an automated reaction to the observed events (actuation networks). As an example, motion detection sensors may trigger lights to turn on after motion has been detected, or sensors monitoring a patient's blood stream may automatically increase the intake of sugars in the event of low-sugar-level detection. In actuation networks, in order to guarantee the robustness of the decision mechanism, it is critical to improve the accuracy and reduce the probability of false alarms.

While robustness may be achieved by pursuing a multimodal approach that involves multiple consistency checks before any actuation decision is made, robustness depends, to a high degree, on the availability of monitoring information. In order to evaluate a specific event, one needs to have sufficient observations of the event. On the other hand, the number of available observations is directly related to the number of sensors able to sense a particular event. Hence, to improve the robustness of the system, one needs to increase the availability of the collected information.

The availability of monitoring information can be measured by computing the *coverage* of the *FoI*, achieved by the sensor network deployment. Coverage quantifies how well an *FoI* is monitored¹. The coverage problem has been studied under different objectives, depending on the requirements and constraints of the applications. If the location of the deployed sensors can be preselected, the coverage problem reduces to the problem of finding the optimal placement for sensors such that a target coverage is met [Kar and Banerjee 2003; Poduri and Sukhatme 2004].

However, for large sensor networks, it is impractical to perform deterministic coverage of the *FoI*, since the number of sensors that need to be placed is often prohibitively large. Instead, sensors are deployed in the field of interest according to a preselected distribution. For stochastically deployed sensor networks, the coverage problem quantifies how well the *FoI* is monitored when a number of sensors are deployed according to a known distribution. This problem is also known as the *stochastic coverage problem* [Koushanfar et al. 2001; Meguerdichian et al. 2001; Liu and Towsley 2004; Miorandi and Altman 2005; Xing et al. 2005]. In this article, we analyze the following stochastic coverage problem. Given a planar *FoI* and N sensors deployed according to a known distribution, compute the fraction of the *FoI* that is covered by at least k sensors ($k \geq 1$). The problem can also be rephrased as follows: given an *FoI* and a sensor distribution, how many sensors must be deployed in order for every point in the field of interest to be covered by at least k sensors with a probability p (k -coverage problem) [Xing et al. 2005].

¹Once the information has been collected by the sensors, an additional mechanism known as *data aggregation* [Krishnamachari et al. 2002] is required to timely communicate the available information for processing. We do not address the aggregation problem in this article.

1.1 Our Contributions

In this article, we make the following contributions. We formulate the problem of coverage in sensor networks as a set intersection problem. We use results from integral geometry to derive analytical expressions quantifying the coverage achieved by stochastic deployment of sensors into a planar field of interest. Compared to previous analytical results [Liu and Towsley 2004; Poduri and Sukhatme 2004; Miorandi and Altman 2005], our formulation allows us to consider a heterogeneous sensing model, where sensors need not have an identical sensing capability. In addition, our approach is applicable to scenarios where the sensing area of a sensor does not follow the unit disk model, but has any arbitrary shape. To the best of our knowledge, only Miorandi and Altman [2005] have considered a heterogeneous sensing model, though obtaining results that eventually only incorporate the mean value of the sensing range in the coverage computation. Furthermore, the formulation in Miorandi and Altman [2005] considered only uniformly deployed sensors. In our approach, sensors can be deployed according to any distribution.

We provide formulas for k -coverage in the case of heterogeneous sensing areas, as well as simplified forms in the case of identical sensing areas. We verify our theoretical results by performing extensive simulations that show an almost exact match between our theoretical derivation and simulation. We compare our analytical formulas with previous analytic results [Liu and Towsley 2004; Poduri and Sukhatme 2004; Miorandi and Altman 2005] by computing the Kullback-Leibler distance [Cover and Thomas 1991] and illustrate that our expressions provide a higher accuracy, since they do not suffer from the border effects [Bettstetter and Krause 2001; Bettstetter and Zangl 2002]. Finally, we provide examples of how to use our analytical expressions to compute the number of sensors that need to be deployed in order to cover an FoI with a desired probability.

The rest of the article is organized as follows. In Section 2, we present related work. In Section 3, we state our network model and formulate the coverage problem as a set intersection problem. In Section 4, we derive analytical expressions for coverage for both heterogeneous and homogeneous sensor networks. In Section 5, we validate our analytical expressions by computing coverage via simulation, and provide examples of computing the coverage in randomly deployed sensor networks. In Section 6, we present our conclusions.

2. RELATED WORK

In this section, we describe previous work related to the coverage problem in wireless sensor networks (see Table I for a summary). The coverage problem in wireless sensor networks has been studied in regard to different objectives and metrics. The characteristic attributes that classify different approaches to the coverage problem are deterministic or stochastic sensor deployment, homogeneous or heterogeneous sensing area, additional design constraints such as energy efficiency, minimum number of sensors that need to be deployed, or network connectivity. Based on the objective, the coverage problem formulation varies to reflect the different assumptions and objectives.

Table I. Comparison of Related Work on the Coverage Problem for Sensor Networks, in Terms of Assumptions and Constraints (*Sensor deployment* refers to the deployment method, deterministic or stochastic as well as the prior knowledge about the location of the sensors. *Sensing model* refers to the assumptions about the sensing areas. *Heterogeneous model* refers to whether the analysis supports sensors with heterogeneous sensing capabilities. *Additional constraints* refers to other objectives set, such as connectivity, energy efficiency, or minimization of the number of sensors deployed.)

Reference	Sensor Deployment	Sensing Model
Kar and Banerjee [2003]	Deterministic	Unit disk
Xing et al. [2005]	Known location	Unit disk
Poduri and Sukhatme [2004]	Deterministic	Unit disk
Meguerdichian et al. [2001]	Known location	Any
Koushanfar et al. [2001]	Known location	Any
Liu and Towsley [2004]	Random	Any
Li et al. [2003]	Known location	Any
Miorandi and Altman [2005]	Random	Any
<i>Our work</i>	<i>Stochastic</i>	<i>Any</i>
Reference	Heterogeneous Model	Additional Constraints
Kar and Banerjee [2003]	No	Connectivity
Xing et al. [2005]	No	Connectivity
Poduri and Sukhatme [2004]	No	k -connectivity
Meguerdichian et al. [2001]	Yes	Worst coverage
Koushanfar et al. [2001]	Yes	Best, worst coverage
Liu and Towsley [2004]	No	None
Li et al. [2003]	Yes	Best, worst coverage
Miorandi and Altman [2005]	Yes	None
<i>Our work</i>	<i>Yes</i>	<i>None</i>

Kar and Banerjee [2003] studied the problem of deterministic node placement in order to achieve connected coverage, that is, to sense the *FoI* with the minimum number of sensors, while keeping the sensor network connected. Kar and Banerjee [2003] modeled the sensing area after the unit disk model and considered sensors with identical sensing range. The problem of connected coverage has also been recently studied by Xing et al. [2005]. The authors provided a geometric analysis that related coverage to connectivity and defined the necessary conditions for a network covering an *FoI* to be connected. The conditions for coverage and connectivity were derived based on the assumptions that the sensing area of each node is identical and circular and the location of the nodes is known. The authors extended their algorithms for the case of probabilistic deployment, and also relaxed their assumptions to nonunit disk-sensing areas, by approximating the real sensing area with the biggest possible circular area included in the real sensing area.

Poduri and Sukhatme [2004] studied the problem of deterministic coverage under the additional constraint that each sensor must have at least k neighbors. They proposed a deployment strategy that would maximize the coverage while the degree of each node is guaranteed to be at least k , under the assumption that the sensing range of the sensors is isotropic.

Meguerdichian et al. [2001] studied the problem of coverage as a path exposure problem. Using a generic sensing model and an arbitrary sensor

distribution, they proposed a systematic method for discovering the minimum exposure path, that is, the path along which the network exhibits the minimum *integral* observability². Koushanfar et al. [2001] investigated the problem of best- and worst-case coverage. In their formulation of the coverage problem, given the location of the sensors and a generic sensing model where the sensing ability of each sensor diminishes with distance, the authors used Voronoi diagrams and Delaunay triangulation to compute the path that maximizes the smallest observability (best coverage) and the path that minimizes the observability by all sensors (worst coverage). Li et al. [2003] provided a decentralized and localized algorithm for calculating the best coverage.

Liu and Towsley [2004] studied the problem of stochastic coverage in large scale sensor networks. For a randomly distributed sensor network, the authors provided the fraction of the *FoI* covered by k sensors and the fraction of nodes that can be removed without reducing the covered area, as well as the ability of the network to detect moving objects. The results presented by Liu and Towsley [2004] hold only for randomly (uniformly) deployed networks and under the assumption that the sensing area of each sensor is identical. Furthermore, the analysis presented by Liu and Towsley [2004] suffered from the border effects problem, illustrated in Bettstetter and Krause [2001] and Bettstetter and Zangl [2002]. The results hold asymptotically under the assumption that the *FoI* expands infinitely in the plane, while the density of the sensor deployment remains constant.

Miorandi and Altman [2005] studied the stochastic coverage problem in ad hoc networks in the presence of channel randomness. For a randomly deployed sensor network, the authors analyzed the effects of shadowing and fading to the connectivity and coverage. They showed that, in the case of channel randomness, the coverage problem can still be modeled with the assistance of the spatial Poisson distribution, by using *expected* size of the sensing area of sensors. While the results by Miorandi and Altman [2005] are applicable to heterogeneous sensor network, they hold only for randomly deployed networks, and are impacted from the border effects problem [Bettstetter and Krause 2001; Bettstetter and Zangl 2002], as noted by Miorandi and Altman [2005].

Gupta et al. [2003] studied the problem of selecting the minimum number of sensors from a set of sensors that are randomly (uniformly) deployed such that the *FoI* is covered and the selected sensors form a connected network. The authors provided centralized and decentralized heuristic algorithms that perform within a bound from the optimal solution. The authors assume that the sensing area of the sensors can have any convex shape, and sensors can have heterogeneous capabilities. As a requirement, the position as well as the shape and size of each sensing area must be known after deployment.

Compared to previous work that derives analytical coverage expressions [Liu and Towsley 2004; Poduri and Sukhatme 2004; Miorandi and Altman 2005], our formulation allows us to consider a network model where (a) sensors can be deployed according to *any* distribution, (b) sensors can have a sensing area of *any*

²The integral observability is defined as the aggregate of the time that a target was observable by sensors while traversing a sensor network.

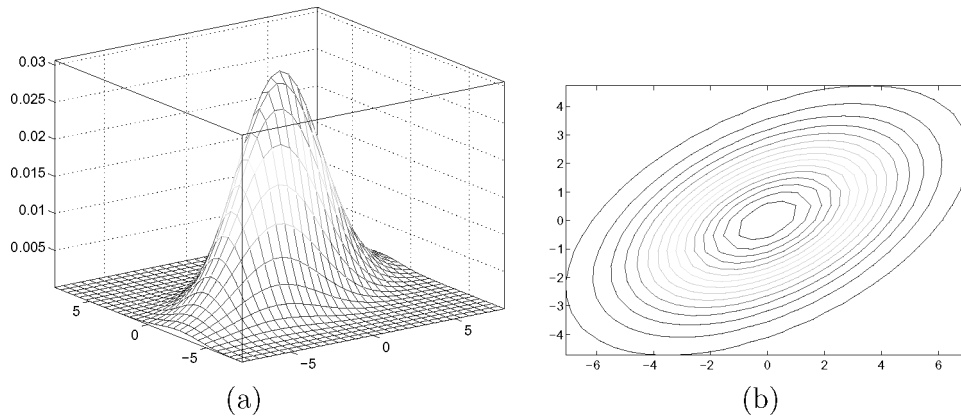


Fig. 1. (a) A two-dimensional Gaussian distribution with mean value $E(X, Y) = [0, 0]$; (b) projection of the Gaussian distribution into the planar field.

arbitrary shape, (c) sensors can have heterogeneous sensing areas. Furthermore, our formulation does not suffer from the border effects problem.

3. NETWORK MODEL, PROBLEM FORMULATION AND BACKGROUND

3.1 Network Model

In many wireless sensor network applications, it is not practical to deploy the sensors deterministically due to the large number of sensors that need to be deployed and/or the type of environment where they are deployed. As an example, sensors may be dropped off an aircraft into a forest in order to monitor environmental parameters such as humidity, temperature, air quality, etc. Furthermore, in many applications, sensors do not remain static even after they have been placed in the *FoI*. Environmental changes, such as air, rain, river streams, etc., may move sensors over time [Szewczyk et al. 2004]. For these types of applications, the relevant coverage question that quantifies the availability of monitoring information is: how many sensors do we need to deploy in order to achieve the desired coverage with a probability higher than a threshold value.

Furthermore, sensors may not be deployed according to a random distribution over the *FoI*. As an example, a subset of points in the *FoI* may be of greater interest than other points and, hence, must be monitored by a larger number of sensors. In such a case, more sensors may be deployed around the critical subset of points. For example, a desired heterogeneous coverage may be achieved by deploying sensors according to a two-dimensional Gaussian distribution. In Figure 1(a), we show the probability density function for a two-dimensional Gaussian distribution with a mean value equal to $E(X, Y) = [0, 0]$. In Figure 1(b), we show the projection of the Gaussian probability density function into the planar field.

Since the sensor deployment distribution may vary, it is desirable to have analytical coverage results that can incorporate any arbitrary sensor distribution.

In our analysis, we study the stochastic coverage problem when sensors are deployed according to any distribution and derive analytical results even in the case of nonuniform sensor distribution.

In addition, it is desirable to develop analytical coverage formulas that hold not only for homogeneous but also for heterogeneous sensor networks. Heterogeneity in the sensing area of sensors may be due to the following reasons. First, the manufacturing process for sensors does not guarantee that sensors are equipped with identical hardware, able to produce an identical sensing model. Furthermore, the heterogeneity of the environment where the sensors are deployed distorts the sensing capabilities of the sensors measured in an ideal environment. Finally, the sensor network may consist of sensors with different sensing capabilities by design (hierarchical sensor networks). We analyze the coverage problem adopting a general sensing model that captures the heterogeneity in the sensing capabilities of sensors.

In this article we adopt the following network model:

- Field of interest (FoI)*. Let \mathcal{A}_0 denote the FoI we want to monitor, with area F_0 and perimeter L_0 . We assume that the FoI is planar and can have any arbitrary shape.
- Sensing area*. Let \mathcal{A}_i denote the sensing area of each sensor s_i , $i = 1 \dots N$, with F_i, L_i denoting the size of the area and perimeter of \mathcal{A}_i . The sensing area can have any arbitrary shape.
- Sensor deployment*. We assume that N sensors are deployed according to a distribution $Y(\mathcal{A}_0)$ and in such a way that they sense some part of the FoI. For sensing, it is not necessary that the sensors are located within the FoI. Instead, we require that sensors can monitor some part of the FoI even if they are located outside of it.

3.2 Problem Formulation

We study the following stochastic coverage problem:

Stochastic coverage problem: Given an FoI \mathcal{A}_0 of area F_0 and perimeter L_0 , sensed by N sensors with each sensor s_i having a sensing area \mathcal{A}_i of size F_i and perimeter L_i deployed in the plane according to a distribution $Y(\mathcal{A}_0)$, compute the fraction of \mathcal{A}_0 that is sensed by at least k sensors, that is, the fraction that is k -covered.

This problem is equivalent to computing the probability that a randomly selected point $P \in \mathcal{A}_0$ is sensed by at least k sensors. The stochastic coverage problem can be mapped to the following set intersection problem:

Set intersection problem: Let S_0 be a fixed bounded set defined as a collection of points in the plane, and let F_0 and L_0 denote the area and perimeter of S_0 . Let N bounded sets S_i ($i = 1 \dots N$) of size F_i and perimeter L_i be dropped in the plane of S_0 according to a distribution $Y(S_0)$ and in such a way that every set S_i intersects with S_0 . Compute the fraction of S_0 where at least k out of the N sets S_i intersect.

In the mapping of the stochastic coverage problem to the set intersection problem, the fixed bounded set S_0 corresponds to the FoI \mathcal{A}_0 . The N bounded

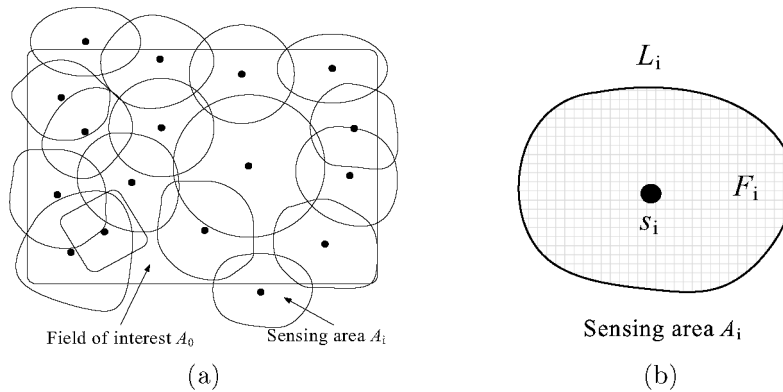


Fig. 2. (a) A heterogeneous sensor network with randomly deployed sensors covering an $FoI A_0$; (b) the sensing area A_i of a sensor s_i .

sets dropped according to the distribution $Y(S_0)$ correspond to the sensing areas of the N sensors deployed according to the distribution $Y(A_0)$. By computing the fraction of the set S_0 , where at least k out of N sets S_i intersect, we equivalently compute the fraction of the FoI that is k -covered³. In Figure 2(a), we show a sensor network randomly deployed over an FoI . In Figure 2(b), we show the sensing area of a sensor s_i . Note that our formulation does not require the FoI to be infinitely extending in the plane. Instead, the FoI has to be a bounded region and, hence, our formulation does not suffer from the border effects problem [Bettstetter and Krause 2001; Bettstetter and Zangl 2002].

The set intersection problem has been a topic of research of integral geometry and geometric probability [Santalo 1936, 1976; Miles 1969; Stoka 1969; Filipescu 1971]. In the following section, we show that the results obtained for the set intersection problem can be used to analyze the coverage problem in wireless sensor networks. Before we provide analytical coverage expressions based on our formulation, we present the relevant background.

3.3 Background on Integral Geometry

In this section, we present relevant background on integral geometry that we use in Section 4 for deriving analytical coverage expressions based on our formulation. Interested readers are referred to Santalo [1936, 1976], Miles [1969], Stoka [1969], and Filipescu [1971] as references to integral geometry. We first introduce the notion of motion for a point P in the plane, defined as follows [Santalo 1976]:

Definition 3.1 (Motion in the plane). Let $P(x_i, y_i)$ denote a point in the Euclidean plane, where x_i, y_i denote Cartesian coordinates. A motion is defined

³Due to their equivalence, A_0 and S_0 as well as the terms *sensing area* and *set* are used interchangeably in the rest of the article.

as a transformation $T : P(x_i, y_i) \rightarrow P'(x'_i, y'_i)$ such that

$$\begin{aligned} x'_i &= x_i \cos \phi - y_i \sin \phi + x, & y'_i &= x_i \sin \phi + y_i \cos \phi + y \\ -\infty < x < \infty, & -\infty < y < \infty, & 0 \leq \phi \leq 2\pi. \end{aligned} \quad (1)$$

Any motion of a point P or a set of points⁴ \mathcal{A} is characterized by the horizontal displacement α , the vertical displacement β , and the rotation ϕ . A group of motions \mathcal{M} denotes a collection (set) of transformations in the Euclidean plane, that is, the respective range for the 3-space (α, β, ϕ) .

To quantify a group of motions \mathcal{M} in the plane, we must define an appropriate measure for the set of transformations of \mathcal{A} determined by \mathcal{M} . Such a measure is called the *kinematic measure* and it must be invariant to the initial position of \mathcal{A} , invariant under translation as well as invariant under inversion of the motion. The need for such invariance will become clear in the example following the definition of kinematic measure.

To define the kinematic measure we must introduce the notion of *kinematic density* for the group of motions \mathcal{M} of a point $P(x, y)$ or set of points \mathcal{A} in the plane. The kinematic density expresses the differential element of motion of a set of points in the plane, and is defined as follows [Santalo 1976]:

Definition 3.2 (Kinematic density). The kinematic density $d\mathcal{A}$ for a group of motions \mathcal{M} in the plane for the set \mathcal{A} , is defined as the differential form

$$d\mathcal{A} = dx \wedge dy \wedge d\phi, \quad (2)$$

where \wedge denotes the exterior product used in exterior calculus [Flanders 1963, 1967; Santalo 1976].

The above definition of kinematic density, using the exterior product form, is the only form up to a constant factor invariant under translation and inversion of motion. Integrating the kinematic density of a set \mathcal{A} over a group of motions \mathcal{M} in the plane yields a measure for the set of motions \mathcal{M} .

Definition 3.3 (Kinematic measure). The kinematic measure m of a set of motions \mathcal{M} in the plane is defined by the integral of the kinematic density $d\mathcal{A}$ over \mathcal{M} :

$$m = \int_{\mathcal{M}} d\mathcal{A}. \quad (3)$$

To provide intuition behind the definition of the kinematic measure and the properties of the kinematic density consider Figure 3(a) showing a fixed set \mathcal{A}_0 and a set \mathcal{A}_1 free to move within the plane. We want to measure the set of motions (transformations) T such that $T(\mathcal{A}_1) \cap \mathcal{A}_0 \neq \emptyset$, that is, to measure the set of transformations $T(\mathcal{A}_1)$ such that the two sets intersect. This measure is the integral of $d\mathcal{A}_1$ over all points $P'(x, y)$ and all angles ϕ such that $T(\mathcal{A}_1) \cap \mathcal{A}_0 \neq \emptyset$.

The invariant under the translation property states that, for any transformation $T'(\mathcal{A}_0)$, the measure of the set of motions T such that $T(\mathcal{A}_1) \cap T'(\mathcal{A}_0) \neq \emptyset$

⁴In the case of a set of points, the set can be represented by a single point O based on which all other points are determined.

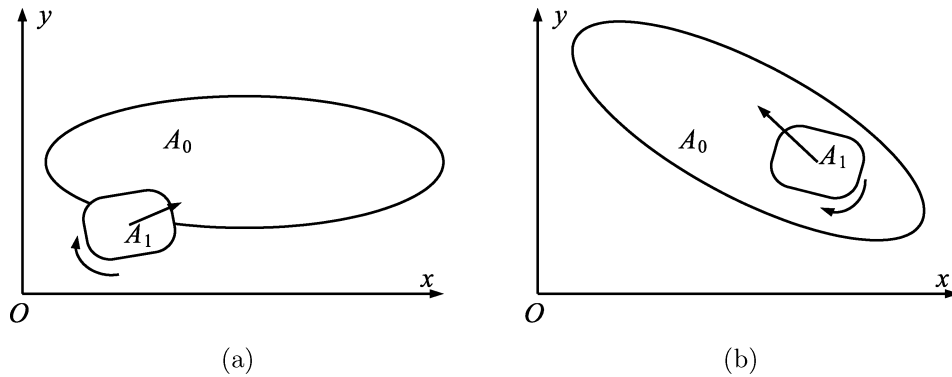


Fig. 3. (a) Set \mathcal{A}_1 is free to move within the plane in such a way that it intersects with fixed set \mathcal{A}_0 . (b) Fixed set \mathcal{A}_0 has a different initial orientation and position. The measure of the set of positions of \mathcal{A}_1 such that it intersects \mathcal{A}_0 , expressed via the kinematic density, is the same regardless of the initial configuration of the two sets. The measure is invariant to translations and rotations of any of the two sets.

must be equal to the measure of the set of motions such that $T(\mathcal{A}_1) \cap \mathcal{A}_0 \neq \emptyset$. Similarly the measure must be invariant to any translations of set \mathcal{A}_1 . Furthermore, the measure is invariant to the order by which we consider the possible motions of the set \mathcal{A}_1 , or the initial positioning of sets $\mathcal{A}_0, \mathcal{A}_1$ [Santalo 1976]. Figure 3(b) shows a different positioning and orientation of the fixed set \mathcal{A}_0 that could be due to the application of a translation or a different initial positioning.

The quotient of the measure of a group of motions Z over the measure of a group of motions \mathcal{M} in the plane, where $Z \subseteq \mathcal{M}$, yields the probability $p(Z)$ for that group of motions to occur:

$$p(Z) = \frac{m(Z)}{m(\mathcal{M})}. \quad (4)$$

The kinematic measure allows us to compute the geometric probability for a specific set configuration to occur, as depicted in (4). Equation (4), is used in our formulation to derive the fraction of the *FoI* covered by a sensor deployment, as illustrated in the following section.

4. ANALYTICAL EVALUATION OF COVERAGE IN HETEROGENEOUS SENSOR NETWORKS

In this section, we derive analytical expressions for stochastic coverage in heterogeneous sensor networks. We first study the coverage problem for the case where only one sensor is deployed, by studying the intersection of two sets in a plane. We initially consider a sensor with a sensing area of convex shape. When the sensing area is convex, only the size and perimeter of the sensing area are required to compute coverage. When the sensing area has a nonconvex shape, additional information such as the decomposition of the sensing area to a union of disjoint convex shapes is required. In Section 4.3, we extend our results for nonconvex sensing areas.

We modify our analytical formulas for the case where the sensor is deployed according to an arbitrary distribution. Using the results from the single sensor

deployment, we generalize for the case where multiple sensors are deployed and compute the fraction of the *FoI* covered by at least k sensors, when a total of N sensors are deployed. Finally, we show how we can derive previous analytical results [Liu and Towsley 2004; Poduri and Sukhatme 2004] as specific cases of our model.

4.1 Random Deployment of a Single Sensor

In this section, we analyze the simplest case where a sensor s_1 is randomly deployed in the plane. We assume that s_1 has a convex sensing area \mathcal{A}_1 of size F_1 and perimeter L_1 . We want to compute the fraction of the *FoI* covered by the sensor s_1 . The equivalent set intersection problem is as follows. Let $\mathcal{A}_0, \mathcal{A}_1$ denote two sets in a plane with \mathcal{A}_0 being fixed, while \mathcal{A}_1 can move freely within the plane. Assume that all positions of \mathcal{A}_1 are equiprobable (sensor s_i is deployed at random). Compute the fraction of \mathcal{A}_0 covered by \mathcal{A}_1 .

Let \mathcal{A}_{01} denote the intersection between sets $\mathcal{A}_0, \mathcal{A}_1$. Since $\mathcal{A}_0, \mathcal{A}_1$ are convex, \mathcal{A}_{01} is also convex. The fraction $fr(\mathcal{A}_0)$ of \mathcal{A}_0 covered by \mathcal{A}_1 is computed by normalizing the size of the area of \mathcal{A}_{01} over the size of \mathcal{A}_0 . The intersection area between the two sets $\mathcal{A}_0, \mathcal{A}_1$ can be computed with tools from integral geometry [Santalo 1936, 1976].

To compute $fr(\mathcal{A}_0)$, we randomly select a point $P \in \mathcal{A}_0$. Let $p(P \in \mathcal{A}_1)$ denote the probability that $P \in \mathcal{A}_1$, that is, that point P belongs in the intersection between the sets \mathcal{A}_0 and \mathcal{A}_1 . Integrating $p(P \in \mathcal{A}_1)$ over all $P \in \mathcal{A}_0$ yields the probability that any point of \mathcal{A}_0 belongs to \mathcal{A}_1 . Since all points are equiprobable, integration of $p(P \in \mathcal{A}_1)$ over all $P \in \mathcal{A}_0$ also computes the area F_{01} of the intersection set between $\mathcal{A}_0, \mathcal{A}_1$. Normalizing F_{01} over the F_0 yields the desired fraction $fr(\mathcal{A}_0)$. The following theorem holds for convex sets, and will be extended in Section 4.3 for the case of nonconvex sets [Santalo 1976].

THEOREM 4.1. *Let \mathcal{A}_0 be a fixed convex set of area F_0 and perimeter L_0 , and let \mathcal{A}_1 be a convex set of area F_1 and perimeter L_1 , randomly dropped in the plane in such a way that it intersects with \mathcal{A}_0 . The probability that a randomly selected point $P \in \mathcal{A}_0$ is covered by \mathcal{A}_1 is given by*

$$p(P \in \mathcal{A}_1) = \frac{2\pi F_1}{2\pi(F_0 + F_1) + L_0 L_1}. \quad (5)$$

PROOF. According to (4), in order to compute the probability that P is covered by \mathcal{A}_1 , we need to compute the quotient of the measure of all motions of \mathcal{A}_1 such that $P \in \mathcal{A}_1$, over the measure of the set of motions of \mathcal{A}_1 such that $\mathcal{A}_0 \cap \mathcal{A}_1 \neq \emptyset$. The latter represents all possible positions where \mathcal{A}_1 can be dropped (recall that as a constraint, we require that \mathcal{A}_1 always intersects \mathcal{A}_0). We now provide the computation of the two measures, also sketched in [Santalo 1936, 1976]:

$$\begin{aligned} m(\mathcal{A}_1 : P \in \mathcal{A}_0 \cap \mathcal{A}_1) &\stackrel{(i)}{=} \int_{P \in \mathcal{A}_0 \cap \mathcal{A}_1} d\mathcal{A}_1 \\ &\stackrel{(ii)}{=} \int_{P \in \mathcal{A}_1} d\mathcal{A}_1 \end{aligned}$$

$$\stackrel{\text{(iii)}}{=} \int_{P \in \mathcal{A}_1} dx \wedge dy \int_0^{2\pi} d\phi \stackrel{\text{(iv)}}{=} 2\pi F_1. \quad (6)$$

In (i), we integrate the kinematic density $d\mathcal{A}_1$ of set \mathcal{A}_1 over all motions of \mathcal{A}_1 such that $P \in \mathcal{A}_0 \cap \mathcal{A}_1$. Since by assumption $P \in \mathcal{A}_0$ and \mathcal{A}_0 is fixed, we only need to integrate over all $P \in \mathcal{A}_1$. In (ii), we integrate $d\mathcal{A}_1$ over all motions of \mathcal{A}_1 such that $P \in \mathcal{A}_1$. In (iii), we express the kinematic density as its differential product form, and consider all possible rotations of \mathcal{A}_1 such that $P \in \mathcal{A}_1$. In (iv), the integral of $dx \wedge dy$ over all $P \in \mathcal{A}_1$ is equal to the area F_1 of \mathcal{A}_1 . The integral of $d\phi$ over all ϕ is equal to 2π since \mathcal{A}_1 can freely rotate around its reference point, leading to the value of $2\pi F_1$.

The result in (6) is intuitive. Given a fixed point P , the number of translation motions of the set \mathcal{A}_1 that can include P , is equal to the area F_1 of \mathcal{A}_1 . For each position of \mathcal{A}_1 that includes P , we can rotate \mathcal{A}_1 a total of 2π positions before we repeat the initial configuration. Hence, the measure of positions of \mathcal{A}_1 such that $P \in \mathcal{A}_1$ under both rotation and translation is equal to $2\pi F_1$.

Let P be a randomly selected point of the fixed set \mathcal{A}_0 . All possible positions of \mathcal{A}_1 that include P can be obtained by translating \mathcal{A}_1 according to the vector v , and rotating \mathcal{A}_1 by $\phi \in [0, 2\pi]$. The measure of all translation is F_1 , while the measure of all rotations is 2π ; hence the measure of all positions such that $P \in \mathcal{A}_1$ is $2\pi F_1$.

We now compute the measure of all motions of \mathcal{A}_1 such that $\mathcal{A}_0 \cap \mathcal{A}_1 \neq \emptyset$:

$$\begin{aligned} m(\mathcal{A}_1 : \mathcal{A}_0 \cap \mathcal{A}_1 \neq \emptyset) &\stackrel{\text{(i)}}{=} \int_{\mathcal{A}_0 \cap \mathcal{A}_1 \neq \emptyset} d\mathcal{A}_1 \\ &\stackrel{\text{(ii)}}{=} \int_{\mathcal{A}_0 \cap \mathcal{A}_1 \neq \emptyset} dx \wedge dy \wedge d\phi \\ &\stackrel{\text{(iii)}}{=} \int_0^{2\pi} (F_0 + F_1 + 2F_{01}) d\phi \\ &\stackrel{\text{(iv)}}{=} 2\pi(F_0 + F_1) + L_0 L_1. \end{aligned} \quad (7)$$

In (i), we integrate the kinematic density $d\mathcal{A}_1$ of set \mathcal{A}_1 over all motions of \mathcal{A}_1 such that $\mathcal{A}_0 \cap \mathcal{A}_1 \neq \emptyset$. In (ii), we write the kinematic density in its expanded differential form as defined in (2). In (iii), we compute the area between \mathcal{A}_0 , \mathcal{A}_1 which is called *mixed area of Minkowski* and integrate over all possible rotations. The integration yields the desired result. Proofs of (iii), (iv) are provided in the Appendix.

Given the two measures (6), (7), we can compute the probability $p(P \in \mathcal{A}_1)$ as

$$p(P \in \mathcal{A}_1) = \frac{m(\mathcal{A}_1 : P \in \mathcal{A}_0 \cap \mathcal{A}_1)}{m(\mathcal{A}_1 : \mathcal{A}_0 \cap \mathcal{A}_1 \neq \emptyset)} = \frac{2\pi F_1}{2\pi(F_0 + F_1) + L_0 L_1}. \quad \square \quad (8)$$

Note that $p(P \in \mathcal{A}_1)$ is only dependent on the area and the perimeter of the convex sets that intersect and not on the shape of those sets. Hence, there can be sets of arbitrary shapes as long as they are convex. In Section 4.3, we will generalize (8) for nonconvex sets, corresponding to nonconvex sensing areas.

Based on Theorem 4.1, we can now compute the fraction $fr(\mathcal{A}_0)$ of \mathcal{A}_0 covered by \mathcal{A}_1 , stated in the following lemma.

LEMMA 4.2. *The fraction $fr(\mathcal{A}_0)$ of a fixed convex set \mathcal{A}_0 of area F_0 and perimeter L_0 that is covered by a convex set \mathcal{A}_1 of area F_1 and perimeter L_1 , when \mathcal{A}_1 is randomly dropped in the plane in such a way that it intersects \mathcal{A}_0 , is given by*

$$fr(\mathcal{A}_0) = \frac{2\pi F_1}{2\pi(F_0 + F_1) + L_0L_1}. \quad (9)$$

PROOF. In Theorem 4.1 we showed the probability that a randomly selected point $P \in \mathcal{A}_0$ also belongs to \mathcal{A}_1 when \mathcal{A}_1 is randomly dropped in the plane so that it intersects with \mathcal{A}_0 . Integrating (8) over all points $P \in \mathcal{A}_0$ provides the size of the area F_C covered by \mathcal{A}_1 :

$$\begin{aligned} F_C &= \int_{P \in \mathcal{A}_0} p(P \in \mathcal{A}_1) dP \stackrel{(i)}{=} p(P \in \mathcal{A}_1) \int_{P \in \mathcal{A}_0} dP \\ &\stackrel{(ii)}{=} p(P \in \mathcal{A}_1) F_0 \stackrel{(iii)}{=} \frac{2\pi F_0 F_1}{2\pi(F_0 + F_1) + L_0L_1}. \end{aligned} \quad (10)$$

In (i), the probability $p(P \in \mathcal{A}_1)$ is independent of the coordinates of P . In (ii), integrating dP over all $P \in \mathcal{A}_0$ yields the size F_0 of \mathcal{A}_0 . In (iii), we substitute $p(P \in \mathcal{A}_1)$ from (8). Normalizing F_C by F_0 yields

$$fr(\mathcal{A}_0) = \frac{F_C}{F_0} = \frac{2\pi F_0 F_1}{2\pi(F_0 + F_1) + L_0L_1} \frac{1}{F_0} = p(P \in \mathcal{A}_1). \quad \square \quad (11)$$

4.2 Deployment of a Single Sensor According to a Distribution $F(\mathcal{A}_0)$

In this section, we consider the problem of computing the coverage achieved by a single sensor when the sensor deployment in the plane follows some nonuniform distribution $F(\mathcal{A}_0)$, with a probability density function $f(x, y)$. As an example, the distribution of the sensor may follow a zero-mean two-dimensional Gaussian distribution around the center of \mathcal{A}_0 , as illustrated in Figure 1. This scenario may apply, for instance, when the sensors are dropped in groups above target points and disperse around the target points.

In the case of a nonuniform sensor distribution, the problem of coverage can also be mapped to the set intersection problem. As in the case of a random distribution, there is a fixed set \mathcal{A}_0 that represents the FoI , and a “free” set \mathcal{A}_1 that is dropped into the plane according to the nonuniform distribution $F(\mathcal{A}_0)$ and in such a way that it intersects with \mathcal{A}_0 . We want to calculate the fraction $fr(\mathcal{A}_0)$ of \mathcal{A}_0 covered by \mathcal{A}_1 .

In order to compute $fr(\mathcal{A}_0)$, in the case of a nonuniform distribution, we repeat the same process as in the uniform distribution. First, we randomly select a point $P \in \mathcal{A}_0$ and compute the probability that P also belongs to \mathcal{A}_1 . This probability is again computed as the quotient between the measures in (6) and (7). However, these measures are now calculated as weighted functions of the probability density function $f(x, y)$.

THEOREM 4.3. *Let \mathcal{A}_0 be a fixed convex set of area F_0 and perimeter L_0 , and let \mathcal{A}_1 be a convex set of area F_1 and perimeter L_1 , dropped into the plane according to a distribution $F(\mathcal{A}_0)$ and in such a way that it intersects with \mathcal{A}_0 . The probability that a randomly selected point $P \in \mathcal{A}_0$ is covered by \mathcal{A}_1 is given by*

$$p(P \in \mathcal{A}_1) = \frac{2\pi \int_{P \in \mathcal{A}_1} f(x, y) dx \wedge dy}{\int_{\mathcal{A}_0 \cap \mathcal{A}_1 \neq \emptyset} f(x, y) dx \wedge dy \wedge d\phi}. \quad (12)$$

PROOF. The measure of all positions of set \mathcal{A}_1 that include point P is equal to

$$\begin{aligned} m(\mathcal{A}_1 : P \in \mathcal{A}_0 \cap \mathcal{A}_1) &\stackrel{\text{(i)}}{=} \int_{P \in \mathcal{A}_0 \cap \mathcal{A}_1} f(x, y) d\mathcal{A}_1 \\ &\stackrel{\text{(ii)}}{=} \int_{P \in \mathcal{A}_0 \cap \mathcal{A}_1} f(x, y) dx \wedge dy \wedge d\phi \\ &\stackrel{\text{(iii)}}{=} \int_{P \in \mathcal{A}_1} f(x, y) dx \wedge dy \int_0^{2\pi} d\phi \\ &\stackrel{\text{(iv)}}{=} 2\pi \int_{P \in \mathcal{A}_1} f(x, y) dx \wedge dy. \end{aligned} \quad (13)$$

In (i), we integrate the kinematic density of \mathcal{A}_1 over all motions of \mathcal{A}_1 such that $P \in \mathcal{A}_1 \cap \mathcal{A}_0$, weighted over the probability density function $f(x, y)$ of the sensor deployment. In (ii), we expand $d\mathcal{A}_1$ according to 2. In (iii), we integrate over all angles ϕ such that $P \in \mathcal{A}_1$ ⁵. In (iv), we substitute the integral over all angles ϕ with 2π . The measure of all positions of set \mathcal{A}_1 such that $\mathcal{A}_0 \cap \mathcal{A}_1 \neq \emptyset$ is equal to

$$\begin{aligned} m(\mathcal{A}_1 : \mathcal{A}_0 \cap \mathcal{A}_1 \neq \emptyset) &\stackrel{\text{(i)}}{=} \int_{\mathcal{A}_0 \cap \mathcal{A}_1 \neq \emptyset} f(x, y) d\mathcal{A}_1 \\ &\stackrel{\text{(ii)}}{=} \int_{\mathcal{A}_1 \neq \emptyset} f(x, y) dx \wedge dy \wedge d\phi. \end{aligned} \quad (14)$$

In (i), we integrate the kinematic density of \mathcal{A}_1 over all motions of \mathcal{A}_1 such that $\mathcal{A}_1 \cap \mathcal{A}_0 \neq \emptyset$, weighted over the probability density function $f(x, y)$ of the sensor deployment. In (ii), we expand $d\mathcal{A}_1$, according to (2). The probability that $p(P \in \mathcal{A}_1)$ is equal to the quotient of the two measures is

$$p(P \in \mathcal{A}_1) = \frac{m(\mathcal{A}_1 : P \in \mathcal{A}_0 \cap \mathcal{A}_1)}{m(\mathcal{A}_1 : \mathcal{A}_0 \cap \mathcal{A}_1 \neq \emptyset)} = \frac{2\pi \int_{P \in \mathcal{A}_1} f(x, y) dx \wedge dy}{\int_{\mathcal{A}_0 \cap \mathcal{A}_1 \neq \emptyset} f(x, y) dx \wedge dy \wedge d\phi}. \quad (15)$$

Based on Lemma 4.2, the fraction of \mathcal{A}_0 covered by \mathcal{A}_1 is equal to $p(P \in \mathcal{A}_1)$. \square

We now derive expressions for coverage in the general case where sensors do not have convex sensing areas.

⁵Since P is selected from \mathcal{A}_0 , $P \in \mathcal{A}_0 \cap \mathcal{A}_1$ is equivalent to $P \in \mathcal{A}_1$.

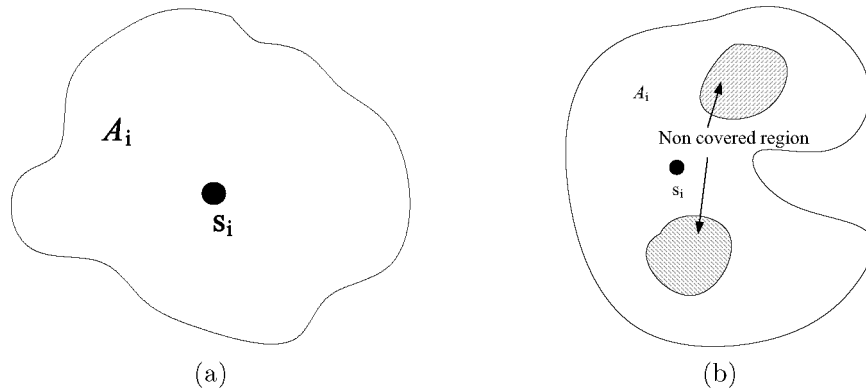


Fig. 4. Nonconvex sensing areas. (a) A rigid nonconvex sensing area, (b) nonconvex sensing area with obstructed regions.

4.3 Random Deployment of Single Sensor with Nonconvex Sensing Area

In our analysis so far, we have assumed the sensing area of the sensors deployed has a convex shape and is bounded by a single curve. However, the shape of the sensing area may not necessarily be convex, or it may consist of multiple separate regions due to obstacles, such as walls pillars, trees, etc. In Figure 4(a), we show the a nonconvex sensing area bounded by a single curve. In Figure 4(b), we show a sensing area with certain areas obstructed by obstacles. Such a nonconvex sensing region is bounded by more than one closed curve. In this section, we compute the coverage achieved by the random deployment of a single sensor with a nonconvex⁶ sensing area.

THEOREM 4.4. *Let \mathcal{A}_0 denote the FoI bounded by a simple⁷ curve, and let \mathcal{A}_1 denote the sensing area of a sensor s_i , with \mathcal{A}_1 being the union of a finite number of separate convex regions \mathcal{A}_1^i , $i = 1 \dots m$, of total area F_1 and total perimeter L_1 . The probability that a randomly selected point $P \in \mathcal{A}_0$ is covered by \mathcal{A}_1 is given by*

$$p(P \in \mathcal{A}_1) = \frac{2\pi F_1}{2\pi(mF_0 + F_1) + L_0L_1}. \quad (16)$$

PROOF. Theorem 4.4 is a special case of the fundamental kinematic formula of Blaschke [1955] that measures a group of motions in the plane for the case where nonconvex areas intersect. In Theorem 4.4, the number of separate convex sets m is defined by the number of closed curves required to bound \mathcal{A}_1 that intersect with the FoI. When the sensing area \mathcal{A}_1 is bounded by a simple curve, as in the case of a compact bounded set, or a convex set, (16) reduces to (5) [Santalo 1976, p. 116]. A detailed proof of Theorem 4.4 is omitted here, but is provided in Santalo [1976], pp. 113–118. \square

⁶The boundary of the sensing area must be piecewise twice differentiable.

⁷A simple curve is defined as a closed curve with no double points [Santalo 1976, p. 113].

Theorem 4.4 allows us to compute the fraction of \mathcal{A}_0 covered by the deployment of a single sensor, when the sensing area of the sensor is nonconvex, by applying Lemma 4.2. Note that to compute $p(P \in \mathcal{A}_1)$ a prior knowledge of a decomposition of the sensing area to a union of disjoint convex areas is required.

4.4 Random Deployment of Multiple Sensors

In this section, we compute the coverage achieved by the random deployment of N sensors, with each sensor s_i having a sensing area \mathcal{A}_i of size F_i and perimeter L_i . As implied by our notations, sensors need not have the same sensing area but can be heterogeneous. We derive formulas for randomly deployed sensors with convex sensing areas. However, equivalent formulas can be obtained for any other distribution and nonconvex shapes by using the results of the coverage achieved by a single sensor deployment, derived in Sections 4.2 and 4.3.

We initially derive the probability $p(S = k)$ that a randomly selected point $P \in \mathcal{A}_0$ is covered by k sensors when N sensors are randomly deployed, using the results from Section 4.1. We then compute the probability that $P \in \mathcal{A}_0$ is covered by at least k sensors, as well as the fraction of \mathcal{A}_0 covered by at least k sensors.

We then simplify our expressions in the case where the sensing areas are identical, and provide formulas for the unit disk model commonly assumed in coverage problems [Liu and Towsley 2004; Poduri and Sukhatme 2004]. Finally, we show how our expressions can be reduced to formulas derived in Liu and Towsley [2004] and Poduri and Sukhatme [2004] under the assumption that the *FoI* is infinite and the deployment density remains constant.

THEOREM 4.5. *Let N sensors be randomly and independently deployed over an *FoI* \mathcal{A}_0 of area F_0 and perimeter L_0 . Let each sensor s_i have a sensing area \mathcal{A}_i of size F_i and perimeter L_i . The probability $p(S = k)$ that a randomly selected point $P \in \mathcal{A}_0$ is covered by exactly k sensors is given by*

$$p(S = k) = \begin{cases} \prod_{i=1}^N \left(\frac{2\pi F_0 + L_0 L_i}{2\pi(F_0 + F_i) + L_0 L_i} \right), & k = 0, \\ \frac{\sum_{i=1}^{\binom{N}{k}} \left(\prod_{j=1}^k (2\pi F_{T(i,j)}) \prod_{z=1}^{N-k} (2\pi F_0 + L_0 L_{G(i,z)}) \right)}{\prod_{r=1}^N (2\pi(F_0 + F_r) + L_0 L_r)}, & k \geq 1. \end{cases} \quad (17)$$

where T is a matrix in which each row j is a “ k -choice” of $[1 \cdots N]$ (a vector of k elements out of N), and G is a matrix in which each row j contains the elements of $[1 \cdots N]$ that do not appear in the j th row of T .

PROOF. In order to prove Theorem 4.5, we map the problem of coverage to the set intersection problem, as illustrated in our problem formulation in Section 3.2. Consider first the case where $k = 0$. When a single sensor s_i is deployed, the probability that it covers a randomly selected point $P \in \mathcal{A}_0$ is given by Theorem

4.1. Hence, the probability $p(P \notin \mathcal{A}_i)$ can be computed as

$$\begin{aligned}
 p(P \notin \mathcal{A}_i) &= 1 - p(P \in \mathcal{A}_i) \\
 &= 1 - \frac{2\pi F_i}{2\pi(F_0 + F_i) + L_0 L_i} \\
 &= \frac{2\pi F_0 + L_0 L_i}{2\pi(F_0 + F_i) + L_0 L_i}. \tag{18}
 \end{aligned}$$

Given that fact that the N sensors are *independently* deployed in the plane so that they cover some part of \mathcal{A}_0 , the probability $p(S = 0)$ that none of the \mathcal{A}_i , $i = 1 \dots N$, covers point P is

$$\begin{aligned}
 p(S = 0) &= p(P \notin \mathcal{A}_1, \dots, P \notin \mathcal{A}_N) \\
 &\stackrel{(i)}{=} \prod_{i=1}^N p(P \notin \mathcal{A}_i) \\
 &\stackrel{(ii)}{=} \prod_{i=1}^N \left(\frac{2\pi F_0 + L_0 L_i}{2\pi(F_0 + F_i) + L_0 L_i} \right). \tag{19}
 \end{aligned}$$

Equality in (i) holds due to the independence in the deployment of the sensors s_i . In (ii), we substitute $p(P \notin \mathcal{A}_i)$ from (18).

In the case where $k \geq 1$, we first need to compute the probability that P is covered by exactly k specific sets. Let T denote a $k \times \binom{N}{k}$ matrix where each row j is a k -choice of the vector $[1 \dots N]$, and let G denote a $(N - k + 1) \times \binom{N}{k}$ matrix where each row j contains the elements of $[1 \dots N]$ that do not appear in the j th row of T . Consider for example, $T(1) = [1 \dots k]$ and $G(1) = [k + 1 \dots N]$. The probability $p(T(1))$ that P is covered by exactly the sets with indexes in the first row of T is given by

$$\begin{aligned}
 p(T(1)) &\stackrel{(i)}{=} p(P \in \mathcal{A}_1, \dots, P \in \mathcal{A}_k, P \notin \mathcal{A}_{k+1}, \dots, P \notin \mathcal{A}_N) \\
 &\stackrel{(ii)}{=} p(P \in \mathcal{A}_1), \dots, p(P \in \mathcal{A}_k) p(P \notin \mathcal{A}_{k+1}), \dots, p(P \notin \mathcal{A}_N) \\
 &\stackrel{(iii)}{=} \frac{2\pi F_1}{2\pi(F_0 + F_1) + L_0 L_1} \dots \frac{2\pi F_k}{2\pi(F_0 + F_k) + L_0 L_k} \\
 &\quad \frac{2\pi F_0 + L_0 L_{k+1}}{2\pi(F_0 + F_{k+1}) + L_0 L_{k+1}} \dots \frac{2\pi F_0 + L_0 L_N}{2\pi(F_0 + F_N) + L_0 L_N} \\
 &= \frac{\prod_{j=1}^k (2\pi F_j) \prod_{z=k+1}^N (2\pi F_0 + L_0 L_z)}{\prod_{r=1}^N (2\pi(F_0 + F_r) + L_0 L_r)} \\
 &= \frac{\prod_{j=1}^k (2\pi F_{T(1,j)}) \prod_{z=1}^{N-k} (2\pi F_0 + L_0 L_{G(1,z)})}{\prod_{r=1}^N (2\pi(F_0 + F_r) + L_0 L_r)}. \tag{20}
 \end{aligned}$$

In (i), we show which k sets include point P . Due to the independence in the set deployment, in (ii), the intersection of the events in (i) becomes a product of the individual events. In (iii), we substitute the individual probabilities from (8) and (18). In the general case, the probability that the sets with indexes of

the i th row of T cover point P is given by

$$p(T(i)) = \frac{\prod_{j=1}^k (2\pi F_{T(i,j)}) \prod_{z=1}^{N-k} (2\pi F_0 + L_0 L_{G(i,z)})}{\prod_{r=1}^N (2\pi(F_0 + F_r) + L_0 L_r)}. \quad (21)$$

Since we are not interested in a specific choice of sets to cover point P , the probability that $p(S = k)$ is a summation of $p(T(i))$ for all possible k -choices. Summing $p(T(i))$ over all i yields (17):

$$\begin{aligned} p(S = k) &= \sum_{i=1}^{\binom{N}{k}} p(T(i)) \\ &= \sum_{i=1}^{\binom{N}{k}} \left(\frac{\prod_{j=1}^k (2\pi F_{T(i,j)}) \prod_{z=1}^{N-k} (2\pi F_0 + L_0 L_{G(i,z)})}{\prod_{r=1}^N (2\pi(F_0 + F_r) + L_0 L_r)} \right) \\ &= \frac{\sum_{i=1}^{\binom{N}{k}} \left(\prod_{j=1}^k (2\pi F_{T(i,j)}) \prod_{z=1}^{N-k} (2\pi F_0 + L_0 L_{G(i,z)}) \right)}{\prod_{r=1}^N (2\pi(F_0 + F_r) + L_0 L_r)}. \quad \square \quad (22) \end{aligned}$$

Once we have computed $p(S = k)$, we can derive the probability that the randomly selected point P is covered by *at least* k sensors.

LEMMA 4.6. *Let \mathcal{A}_0 be an FoI of size F_0 and perimeter L_0 , and let N sensors with sensing area \mathcal{A}_i of size F_i and perimeter L_i be independently and randomly deployed over \mathcal{A}_0 . The probability that a randomly selected point of \mathcal{A}_0 is covered by at least k sensors is given by*

$$p(S \geq k) = \begin{cases} 1, & k = 0, \\ 1 - \sum_{l=0}^{k-1} \frac{\sum_{i=1}^{\binom{N}{l}} \left(\prod_{j=1}^l (2\pi F_{T(i,j)}) \prod_{z=1}^{N-l} (2\pi F_0 + L_0 L_{G(i,z)}) \right)}{\prod_{r=1}^N (2\pi(F_0 + F_r) + L_0 L_r)}, & k \geq 1. \end{cases} \quad (23)$$

PROOF. Lemma 4.6, holds by observing that

$$p(S \geq k) = 1 - \sum_{l=0}^{k-1} p(l = i), \quad (24)$$

and substituting (17) into (24). \square

Lemma 4.6 allows us to compute the fraction $fr(\mathcal{A}_0)$ covered by at least k sets.

THEOREM 4.7. *The fraction $fr(\mathcal{A}_0)$ of an FoI \mathcal{A}_0 of area F_0 and perimeter L_0 that is covered by at least k sensors, when N sensors of sensing area \mathcal{A}_i of size F_i and perimeter L_i are randomly and independently deployed in the plane in*

such a way that they cover some part of the FoI, is given by

$$fr(\mathcal{A}_0) = \begin{cases} 1, & k = 0, \\ 1 - \sum_{l=0}^{k-1} \frac{\sum_{i=1}^{\binom{N}{l}} \left(\prod_{j=1}^l (2\pi F_{T(i,j)}) \prod_{z=1}^{N-l} (2\pi F_0 + L_0 L_{G(i,z)}) \right)}{\prod_{r=1}^N (2\pi(F_0 + F_r) + L_0 L_r)}, & k \geq 1. \end{cases} \quad (25)$$

PROOF. By mapping the coverage problem to the set intersection problem, the size F_C of the area covered by at least k sensors can be computed by integrating the probability that a randomly selected point $P \in \mathcal{A}_0$ is covered by at least k sets, over all points P :

$$F_C = \int_{P \in \mathcal{A}_0} p(S \geq k) dP = p(P \geq k) \int_{P \in \mathcal{A}_0} dP = p(P \geq k) F_0. \quad (26)$$

Normalizing F_C by F_0 yields the result of Theorem 4.7. \square

The fraction $fr(\mathcal{A}_0)$ covered by at least k sensors is equal to the probability that a randomly selected point P is covered by at least k sensors.

COROLLARY 4.8. *The fraction of \mathcal{A}_0 that is not covered by any sensor when N sensors are randomly deployed is given by*

$$p(S = 0) = \prod_{i=1}^N \left(\frac{2\pi F_0 + L_0 L_i}{2\pi(F_0 + F_i) + L_0 L_i} \right). \quad (27)$$

PROOF. The Corollary follows from Theorem 4.5, for $k = 0$. \square

4.5 Coverage in the Case of Homogeneous Sensing Areas

The analytic expressions derived in Section 4.4 hold for heterogeneous sensor networks where the sensing areas of the sensors are of different sizes and perimeters. In the case of homogeneous sensor networks where for each sensor $s_i, i = 1 \dots N$ $F_i = F$, and $L_i = L$, the coverage expressions can be simplified to expressions involving binomials.

COROLLARY 4.9. *The fraction $fr(\mathcal{A}_0)$ of an FoI \mathcal{A}_0 of area F_0 and perimeter L_0 that is covered by at least k sensors, when N sensors of sensing area A_i of size $F_i = F$ and perimeter $L_i = L$ are randomly and independently deployed in the plane in such a way that they cover some part of FoI, is given by*

$$fr(\mathcal{A}_0) = \begin{cases} 1, & k = 0, \\ 1 - \sum_{l=0}^{k-1} \left(\frac{\binom{N}{l} (2\pi F)^l (2\pi F_0 + L_0 L)^{N-l}}{(2\pi(F_0 + F) + L_0 L)^N} \right), & k \geq 1. \end{cases} \quad (28)$$

PROOF. The corollary holds by substituting $F_{T(i,j)} = F, L_{G(i,j)} = L$ into (25). \square

Note that so far in our computations, the FoI is a bounded region. Previous analytical results for homogeneous sensor networks have required that the FoI

of interest is infinitely expanding in the plane [Liu and Towsley 2004; Poduri and Sukhatme 2004; Miorandi and Altman 2005], and have provided asymptotic formulas of coverage. Under the same assumption and using Corollary 4.9, we can derive the same asymptotic results expressed in the following corollary.

COROLLARY 4.10. *Let N sensors of sensing area \mathcal{A}_i of size $F_i = F$ and perimeter $L_i = L$ be randomly and independently deployed in the plane, in such a way that they cover some part of an FoI \mathcal{A}_0 of size F_0 and perimeter L_0 . If \mathcal{A}_0 expands in the whole plane in such a way such that the sensor density remains a constant ($\frac{N}{F_0} \rightarrow \rho$), the fraction $fr(\mathcal{A}_0)$ covered by at least k sensors is given by*

$$fr(\mathcal{A}_0) \rightarrow \begin{cases} 1, & k = 0, \\ 1 - \sum_{l=0}^{k-1} \left(\frac{(\rho F)^l}{k!} e^{-\rho F} \right), & k \geq 1. \end{cases} \quad (29)$$

PROOF. Let us first compute the probability that exactly k sets intersect in a randomly selected point $P \in \mathcal{A}_0$. Substituting $F_i = F$, $L_i = L$ into (17) yields

$$\begin{aligned} p(S = k) &= \binom{N}{k} \left(\frac{2\pi F}{2\pi(F_0 + F) + L_0 L} \right)^k \left(\frac{2\pi F_0 + L_0 L}{2\pi(F_0 + F) + L_0 L} \right)^{N-k} \\ &= \binom{N}{k} q^k (1 - q)^{N-k}, \end{aligned} \quad (30)$$

where $q = \frac{2\pi F}{2\pi(F_0 + F) + L_0 L}$. The binomial distribution can be approximated by a Poisson distribution when N goes to infinity:

$$\lim_{N \rightarrow \infty} p(S = k) = \frac{(Nq)^k}{k!} e^{-Nq}. \quad (31)$$

As $F_0 \rightarrow \infty$, $\frac{F}{F_0} \rightarrow 0$, and if the sensor deployment density $\frac{N}{F_0} \rightarrow \rho$ where ρ is constant, Nq asymptotically tends to

$$\begin{aligned} \lim_{F_0 \rightarrow \infty, \frac{N}{F_0} \rightarrow \rho} (Nq) &= \lim_{F_0 \rightarrow \infty, \frac{N}{F_0} \rightarrow \rho} \left(\frac{2\pi N F}{2\pi(F_0 + F) + L_0 L} \right) \\ &= \lim_{F_0 \rightarrow \infty, \frac{N}{F_0} \rightarrow \rho} \left(\frac{2\pi N F}{2\pi F_0 \left(1 + \frac{F}{F_0} + \frac{L_0 L}{2\pi F_0} \right)} \right) \\ &= \frac{NF}{F_0} = \rho F, \end{aligned} \quad (32)$$

since $\frac{L_0}{F_0} \rightarrow 0$ regardless of the shape of \mathcal{A}_0 [Santalo 1976]. Substituting (32) into (31) yields

$$p(S = k) \rightarrow \frac{(Nq)^k}{k!} e^{-Nq} = \frac{\left(N \frac{F}{F_0} \right)^k}{k!} e^{-N \frac{F}{F_0}} = \frac{(\rho F)^k}{k!} e^{-\rho F}. \quad (33)$$

Hence, the fraction $fr(\mathcal{A}_0)$ of \mathcal{A}_0 covered by at least k sensors with identical sensing area \mathcal{A}_i , when sensors are deployed randomly with a constant density

ρ , as \mathcal{A}_0 expands in the whole plane is given by

$$\begin{aligned}
 \lim_{N \rightarrow \infty} fr(\mathcal{A}_0) &= \lim_{N \rightarrow \infty} \left(1 - \sum_{l=0}^{k-1} p(S=l) \right) \\
 &= 1 - \lim_{N \rightarrow \infty} \left(\sum_{l=0}^{k-1} p(S=l) \right) = 1 - \sum_{l=0}^{k-1} \left(\lim_{N \rightarrow \infty} p(S=l) \right) \\
 &= \begin{cases} 1, & k=0, \\ 1 - \sum_{l=0}^{k-1} \left(\frac{(\rho F)^l}{l!} e^{-\rho F} \right), & k \geq 1. \quad \square \end{cases} \quad (34)
 \end{aligned}$$

We now validate our theoretical results via simulation.

5. VALIDATION OF THE THEORETICAL RESULTS

In this section, we validate our theoretical results via simulation. We also compare our results with the approximation formulas derived in Liu and Towsley [2004], Poduri and Sukhatme [2004], and Miorandi and Altman [2005]. Our evaluation is done in terms of the Kullback Leibler distance (KL-distance) of the probability density functions (pdfs), which provides a performance comparison in the average sense. Considering the pdf obtained via simulation to be the desired distribution q , we compute the KL-distance of our theoretical formulas and the approximations provided in Liu and Towsley [2004], Poduri and Sukhatme [2004], and Miorandi and Altman [2005]. The KL-distance for two distributions p, q , when q is the desired distribution and p is the true distribution is defined as follows [Cover and Thomas 1991]:

Definition 5.1 (Kullback Leibler distance). The Kullback Leibler distance between a desired distribution q and a true distribution p is equal to

$$KL(p, q) = \sum_{p_i} p_i \log_2 \frac{p_i}{q_i}, \quad (35)$$

where p_i, q_i denote the discrete values of the distributions p, q respectively.

We also compare theory, simulation and approximation results with respect to the total variation distance (TV-distance), a metric that reflects the worst-case performance and is defined as follows:

Definition 5.2 (Total variation distance). The total variation distance between two distributions q, p is the maximum difference between the probabilities that can be assigned to the same event,

$$TV(p, q) = \sup_i \{|p_i - q_i|\}. \quad (36)$$

We validate our formulas for homogeneous networks (sensors have identical sensing area) as well as heterogeneous networks (sensors have different sensing areas).

5.1 Homogeneous Sensor Network—Unit Disk Sensing Area

In our first experiment, we randomly deployed a variable number of sensors with identical sensing area in a circular *FoI* of radius $R = 100$ m. All sensors had

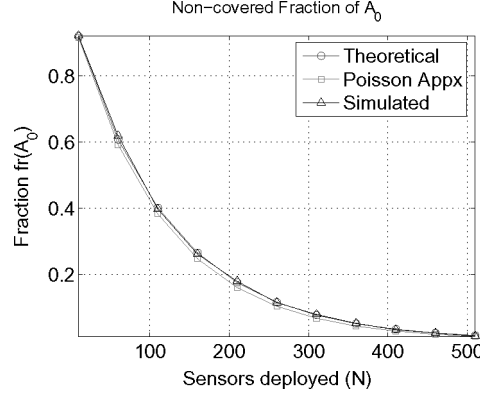


Fig. 5. Fraction $fr(\mathcal{A}_0)$ of \mathcal{A}_0 , that remains noncovered as a function of the number of sensors N that are deployed to monitor the FoI .

a circular sensing area of radius $r = 10$ m. We repeated the random deployment of sensors 100 times and averaged the results. In Figure 5, we show the fraction $fr(\mathcal{A}_0)$ of \mathcal{A}_0 , that remained noncovered as a function of the number of sensors N that are deployed to monitor the FoI . The theoretical formula that computes that desired fraction is obtained from Corollary 4.8 and is equal to

$$\begin{aligned} fr(\mathcal{A}_0) = p(S = 0) &= \prod_{i=1}^N \frac{2\pi F_0 + L_0 L_i}{2\pi(F_0 + F_i) + L_0 L_i} = \prod_{i=1}^N \frac{2\pi F_0 + L_0 L}{2\pi(F_0 + F) + L_0 L} \\ &= \left(\frac{2\pi F_0 + L_0 L}{2\pi(F_0 + F) + L_0 L} \right)^N, \end{aligned} \quad (37)$$

where $F_0 = \pi R^2$, $L_0 = 2\pi R$, $F = \pi r^2$, $L = 2\pi r$. The Poisson approximation of the fraction of \mathcal{A}_0 that is noncovered was given by Liu and Towsley [2004], Poduri and Sukhatme [2004], and Miorandi and Altman [2005]:

$$fr'(\mathcal{A}_0) = p'(S = 0) = e^{-\frac{NF}{F_0}}. \quad (38)$$

We observe that the simulation results verify our theoretical expression, while the Poisson approximation deviates from the simulation results. In Figure 6(a), we show the pdf of the fraction $fr(\mathcal{A}_0)$ covered by exactly k sensors when $N = 300$ sensors with identical sensing areas are randomly deployed. The equivalent sensor density is equal to $\rho = 0.0095$ sensors/m². The same graphs for $N = 500$, $N = 1000$ (densities $\rho = 0.016$ sensors/m², $\rho = 0.032$ sensors/m²) are provided in Figures 6(c) and 7(a), respectively. According to Theorem 4.7, $fr(\mathcal{A}_0)$ is equal to the pdf of the probability that a randomly selected point P is covered by exactly k sensors. Our analytical derivation in Section 4.5, yields

$$fr(\mathcal{A}_0) = p(S = k) = \frac{\binom{N}{k} (2\pi F)^k (2\pi F_0 + L_0 L)^{N-k}}{(2\pi(F_0 + F) + L_0 L)^N}. \quad (39)$$

The Poisson approximation of the fraction of \mathcal{A}_0 that is covered by exactly k sensors is equal to [Liu and Towsley 2004]

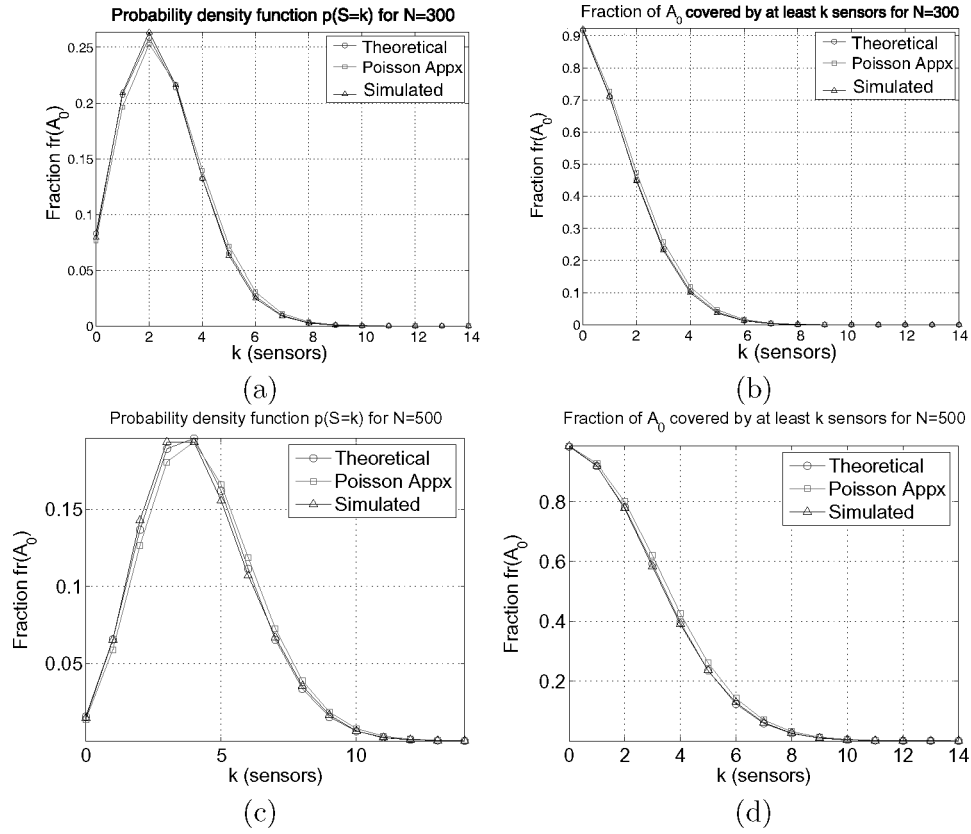


Fig. 6. (a) The pdf of the fraction $fr(A_0)$ covered by exactly k sensors when $N = 300$ sensors with identical sensing areas are randomly deployed. (b) The fraction $fr(A_0)$ covered by at least k sensors when $N = 300$ sensors with identical sensing areas are randomly deployed. (c) The pdf of the fraction $fr(A_0)$ covered by exactly k sensors when $N = 500$ sensors with identical sensing areas are randomly deployed. (d) The fraction $fr(A_0)$ covered by at least k sensors when $N = 500$ sensors with identical sensing areas are randomly deployed.

$$fr'(A_0) = p'(S = k) = \frac{\left(\frac{NF}{F_0}\right)^k}{k!} e^{-\frac{NF}{F_0}}. \quad (40)$$

For the pdf of the number of sensors covering exactly a fraction of the FoI , we computed the KL-distance and TV-distance between the theoretical pdf in (39) from the simulated pdf as well as KL-distance and TV-distance of the Poisson approximated pdf in (40) from the simulated pdf. In Table II, we summarize the comparison of the theoretical pdf and its Poisson approximation. We observe a deviation of the Poisson approximated formula from the simulated results, mainly due to the border effects [Bettstetter and Zangl 2002]. On the other hand, our theoretical pdf is almost identical to a real pdf (the KL-distance is equal to zero when the two distribution compared are identical), showing that our analytical derivation accurately predicts the coverage achieved by the sensor deployment.

Table II. Comparison of KL-Distance and TV-Distance of our Theoretical pdf $p(S = k)$ with the Spatial Poisson Approximation $p'(S = k)$ for Varying Number of Sensors with Identical Sensing Areas, Randomly Deployed in the FoI (The pdf in (39) provides an almost exact match to the desired distribution (the KL-distance is very close to zero), while the pdf in (40) has a higher KL-distance from the desired distribution that grows as N increases. The TV-distance is also significantly smaller using our exact formula compared to the Poisson approximation.)

Number of Nodes (N)	Theoretical Result in (39)		Poisson Approximation in (40)	
	KL-dist. ($\times 10^{-3}$)	TV-dist. ($\times 10^{-3}$)	KL-dist. ($\times 10^{-3}$)	TV-dist. ($\times 10^{-3}$)
300	0.56	14.3	4.2	34.4
500	0.11	6.4	5.9	58.5
700	0.062	4.4	7.1	48.0
1000	0.096	3.6	9.4	52.1
1500	0.01	2.8	13.4	40.6

$R = 100$ m, $r = 10$ m, $F_0 = \pi R^2$, $L_0 = 2\pi$, $F = \pi r^2$, $L_0 = 2\pi r$

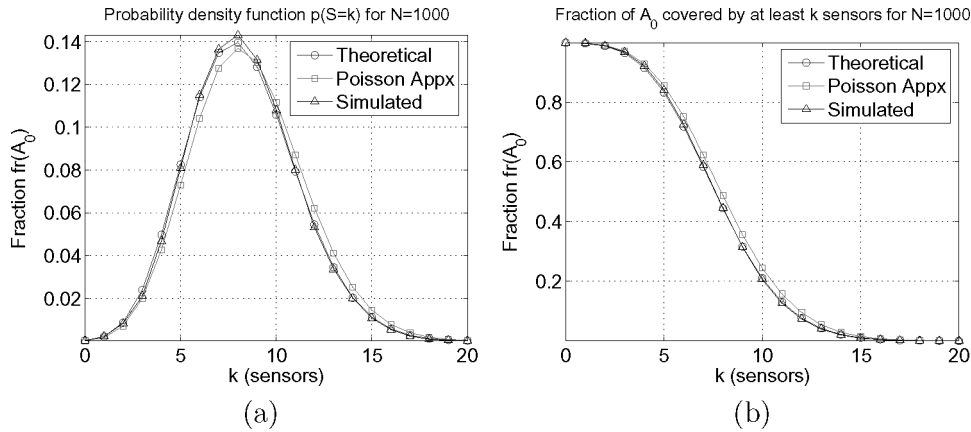


Fig. 7. (a) The pdf of the fraction $fr(\mathcal{A}_0)$ covered by exactly k sensors when $N = 1000$ sensors with identical sensing areas are randomly deployed. (b) The fraction $fr(\mathcal{A}_0)$ covered by at least k sensors when $N = 1000$ sensors with identical sensing areas are randomly deployed.

We also observe that the KL-distance for the Poisson approximation increases with the increase of N . This is due to the fact that, as the number of sensors increases, more sensors will be deployed at the border of the deployment region, and, hence, the border effect becomes more significant. On the other hand, no such pattern occurs for the KL-distance for our theoretical result. In terms of the worst-case performance, the TV-distance using (39) is significantly smaller compared to the TV-distance between the simulation the Poisson approximation in (40).

In Figure 6(b), we show the fraction of \mathcal{A}_0 covered by *at least* k sensors when $N = 300$. The same graphs for $N = 500$, $N = 1000$ are provided in Figures 6(d) and 7(b), respectively. For all graphs in Figures 6, and 7 we show the theoretical results according to our expressions and the simulation values, as well as the Poisson approximation.

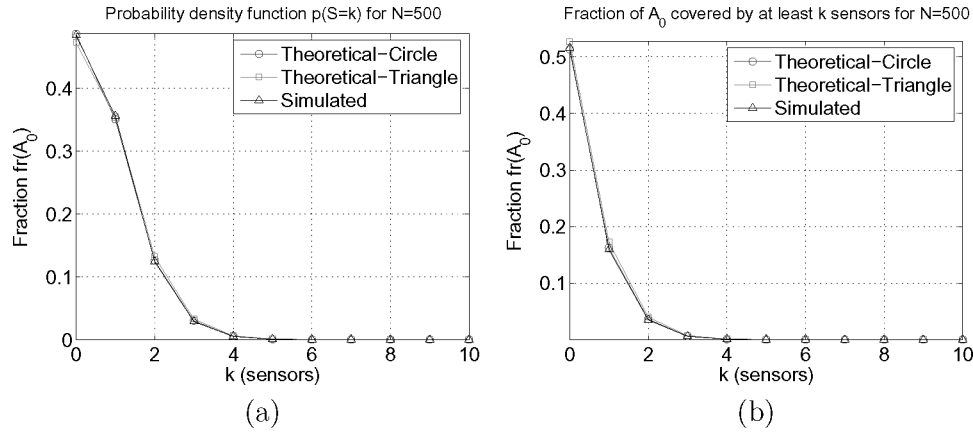


Fig. 8. (a) The pdf of the fraction $fr(\mathcal{A}_0)$ covered by exactly k sensors when $N = 500$ sensors with identical sensing areas are randomly deployed. (b) The fraction $fr(\mathcal{A}_0)$ covered by at least k sensors when $N = 500$ sensors with identical sensing areas are randomly deployed.

5.2 Homogeneous Sensor Networks—Triangular Sensing Area

In our second experiment, we studied the impact of the shape of the sensing area of the sensor to coverage. We randomly deployed 500 sensors in a circular *FoI* of radius 100 m. Each sensor had a triangular sensing area with each side of the triangle being equal to $r = 10$ m. The size of the sensing area of each sensor is equal to $F = r^2 \frac{\sqrt{3}}{4}$ while the perimeter is equal to $L = 3r$. We repeated the experiment 100 times, then computed the coverage probability and averaged the results.

We then repeated the same experiment with sensors having a circular sensing area of size equal to the triangular one, and computed the achieved coverage. For the circular sensing area, the equivalent radius is equal to $r_c = r \frac{3^{\frac{1}{4}}}{\sqrt{4\pi}}$. In Figure 8(a), we compare the pdf of the fraction of \mathcal{A}_0 covered by exactly k sensors obtained via theoretical computation as well as the simulation outcome, for both triangular and circular sensing areas. In Figure 8(b), we show fraction of \mathcal{A}_0 covered by at least k sensors obtained via theoretical computation as well as the simulation outcome, for both triangular and circular sensing areas.

We observe that independent of the shape of the sensing area the theoretical computation using triangular sensing areas is almost equal to the theoretical computation using circular sensing areas. This result shows that, if the number of sensors deployed is relatively large, the coverage achieved does not depend on the shape of the sensing area, but only on the size of the sensing area. Though the circular and the triangular sensing areas have different perimeters, they achieve the same coverage since they have the same size F .

Analyzing formula (23), the coverage probability depends on the fractions $\frac{F}{F_0}$, $\frac{L_0 L}{F_0}$. Since in our experiment the triangular sensing area had the same size as the circular sensing area, the difference in the coverage probability in the two deployments depends only on the fraction $\frac{L_0 L}{F_0}$. However, the difference in the fraction $\frac{L_0 L}{F_0}$ for triangles and circles is negligible with respect to the value of

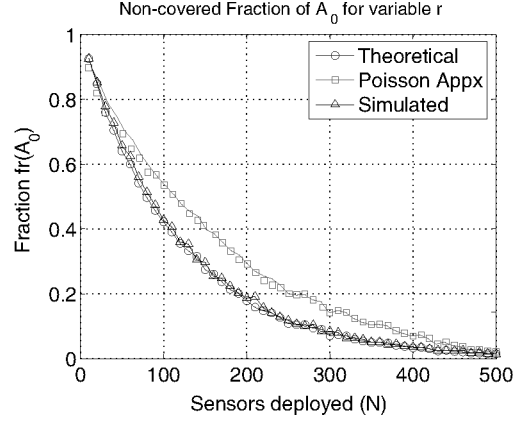


Fig. 9. Fraction $fr(\mathcal{A}_0)$ of \mathcal{A}_0 , that remains noncovered as a function of the number of sensors N that are deployed to monitor the FoI , for the heterogeneous network deployed in the second experiment.

2π , or $(2\pi + \frac{F}{F_0})$ where it is added. Hence, although \mathcal{A}_0 does not extend infinitely; its size is sufficiently large that the impact of the perimeter of the sensing area L is negligible. This would not be the case if F_0 and L were of comparable size, or the perimeters of the sensing areas differed significantly.

The independence of the coverage achieved from the shape of the sensing areas, is also illustrated in the Poisson approximation shown in (31), where the coverage only depends on the size of the area F and not the perimeter L . As F_0 increases, both $\frac{L}{F_0}$ and $\frac{L_0}{F_0}$ tend to zero [Santalo 1976] and, hence, the perimeter of both the FoI and the sensing area do not influence the coverage probability.

5.3 Heterogeneous Sensor Networks

In our second experiment, we considered a hierarchical (heterogeneous) sensor network, where two types of sensors are deployed. Type A has a sensing area of disk shape with a sensing range $r_A = 10$ m, while type B has a sensing area of disk shape with a sensing range of $r_B = 15$ m. We randomly deployed an equal number $N_A = N_B = \frac{N}{2}$ of sensors of each type over a circular FoI of size $F_0 = \pi R^2$ where $R = 100$ m. In Figure 9, we show the fraction $fr(\mathcal{A}_0)$ of \mathcal{A}_0 , that remains noncovered as a function of the number of sensors N that are deployed to monitor the FoI . The theoretical formula that computes that is equal to

$$fr(\mathcal{A}_0) = p(S = 0) = \prod_{i=1}^N \frac{2\pi F_0 + L_0 L_i}{2\pi(F_0 + F_i) + L_0 L_i}, \quad (41)$$

where $F_0 = \pi R^2$, $L_0 = 2\pi R$, $F_i = \pi r_i^2$, $L = 2\pi r_i$. The Poisson approximation of the fraction of \mathcal{A}_0 that is noncovered was illustrated in Miorandi and Altman

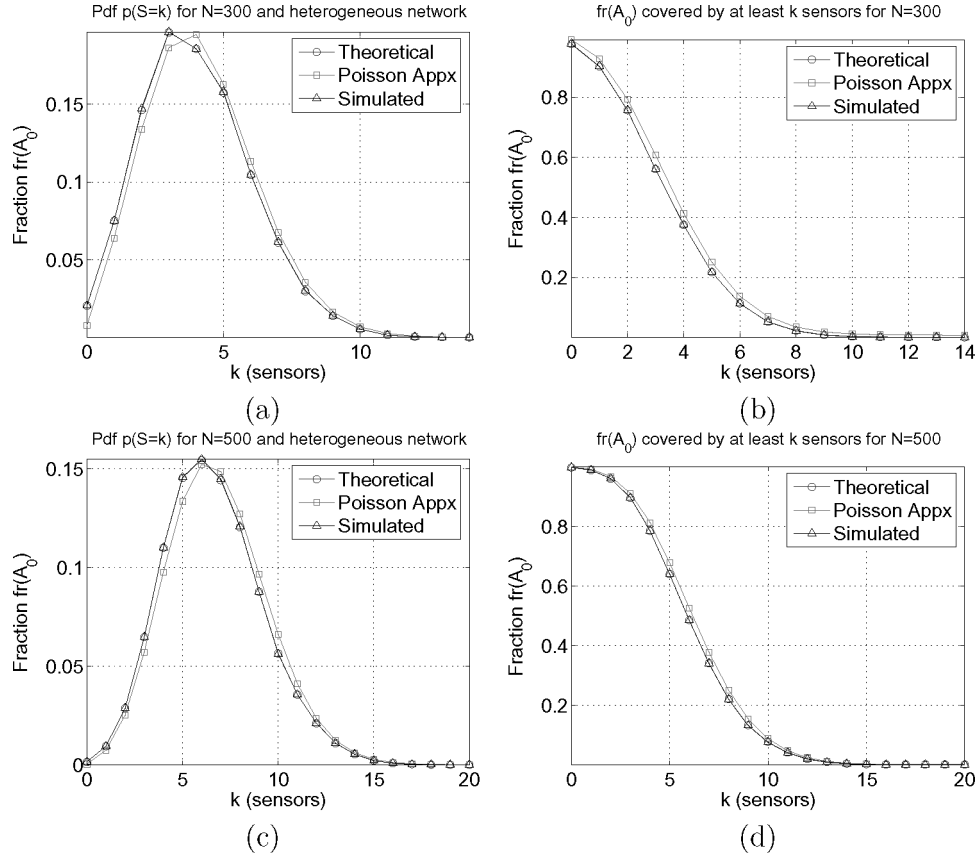


Fig. 10. Heterogeneous sensor network, with FoI being a disk of radius $R = 100$ m. An equal number of two types of sensors are deployed; Type A has a sensing area of a disk shape with radius $r_A = 10$ m, while type B has a sensing area of a disk shape with $r_B = 15$ m. (a) The pdf of the fraction $fr(A_0)$ covered by exactly k sensors when $N = 300$ sensors. (b) The fraction $fr(A_0)$ covered by at least k sensors when $N = 300$ sensors. (c) The pdf of the fraction $fr(A_0)$ covered by exactly k sensors when $N = 500$ sensors. (d) The fraction $fr(A_0)$ covered by at least k sensors when $N = 500$ sensors.

[2005], and is given by

$$fr'(A_0) = p'(S = 0) = e^{-\frac{NE[F]}{F_0}}. \quad (42)$$

where $E[F] = \pi E[r^2]$ denotes the expected value of the sensing area of the sensors deployed.

We observe that the simulation results verify our theoretical expression, while the Poisson approximation deviates from the simulation results. In Figure 10(a), we show the pdf of the fraction $fr(A_0)$ covered by exactly k sensors when $N = 300$ sensors are randomly deployed. The equivalent sensor density is equal to $\rho = 0.0095$ sensors/m². The same graphs for $N = 500$, $N = 1000$ (densities $\rho = 0.016$ sensors/m², $\rho = 0.032$ sensors/m²) are provided in Figures 10(c) and 11(a), respectively. According to Theorem 4.7, $fr(A_0)$ is equal

Table III. Heterogeneous Sensor Network, with FoI Being a Disk of Radius $R = 100$ m. (An equal number of two types of sensors are deployed; Type A has a sensing area of a disk shape with radius $r_A = 10$ m, while type B has a sensing area of a disk shape with $r_B = 15$ m. The table compares the KL-distance and TV-distance of our theoretical pdf $p(S = k)$ with the spatial Poisson approximation $p'(S = k)$ for varying number of sensors with identical sensing areas, randomly deployed in the FoI . The pdf in (43) provides an almost exact match to the desired distribution (the KL-distance is very close to zero), while the pdf in (44) has a significant distance from the desired distribution that grows as N increases.)

Number of Nodes (N)	Theoretical Result in (43)		Poisson Approximation in (44)	
	KL-dist. ($\times 10^{-3}$)	TV-dist. ($\times 10^{-3}$)	KL-dist. ($\times 10^{-3}$)	TV-dist. ($\times 10^{-3}$)
300	0.86	14.7	2.2	36.3
500	1.4	18.3	6.9	38.4
700	0.062	7.8	8.4	49.4
1000	0.096	10.9	12.3	59.6
1500	0.15	11.5	15.7	65.2

$R = 100$ m, $r_A = 10$ m, $r_B = 15$ m, $F_0 = \pi R^2$, $L_0 = 2\pi$
 $F_A = \pi r_A^2$, $L_A = 2\pi r_A$, $F_B = \pi r_B^2$, $L_B = 2\pi r_B$, $N_A = N_B = \frac{N}{2}$

to the pdf $p(S = k)$ of the probability that a randomly selected point P is covered by exactly k sensors. Our analytical derivation in Section 4.4 yields

$$fr(\mathcal{A}_0) = p(S = k) = \begin{cases} \prod_{i=1}^N \left(\frac{2\pi F_0 + L_0 L_i}{2\pi(F_0 + F_i) + L_0 L_i} \right), & k = 0, \\ \frac{\sum_{i=1}^{\binom{N}{k}} \left(\prod_{j=1}^k (2\pi F_{T(i,j)}) \prod_{z=1}^{N-k} (2\pi F_0 + L_0 L_{G(i,z)}) \right)}{\prod_{r=1}^N (2\pi(F_0 + F_r) + L_0 L_r)}, & k \geq 1. \end{cases} \quad (43)$$

The Poisson approximation of the fraction of \mathcal{A}_0 that is covered by exactly k sensors is equal to

$$fr'(\mathcal{A}_0) = p'(S = k) = \frac{\left(\frac{NE[F]}{F_0} \right)^k}{k!} e^{-\frac{NE[F]}{F_0}}. \quad (44)$$

For the pdf of the number of sensors covering exactly a fraction of the FoI in the heterogeneous case, we again computed the KL-distance and TV-distance between the theoretical pdf in (43) from the simulated pdf as well as the KL-distance and TV-distance of the Poisson approximated pdf in (43) from the simulated pdf. In Table III, we summarize the comparison of the theoretical pdf and its Poisson approximation. As in the case of the homogeneous network, we observe a higher deviation of the Poisson approximated formula from the simulated results. This deviation is not only due to the border effects [Bettstetter and Krause 2001; Bettstetter and Zangl 2002], but also due to the use of the expected size of the sensing area of the sensors in the Poisson approximated formula. On the other hand, our theoretical pdf is almost identical to a real pdf, showing that our analytical derivation accurately predicts the coverage achieved by the sensor deployment.

As in the case of the homogeneous sensor network, we also observe that the KL-distance and TV-distance for the Poisson approximation increases with the

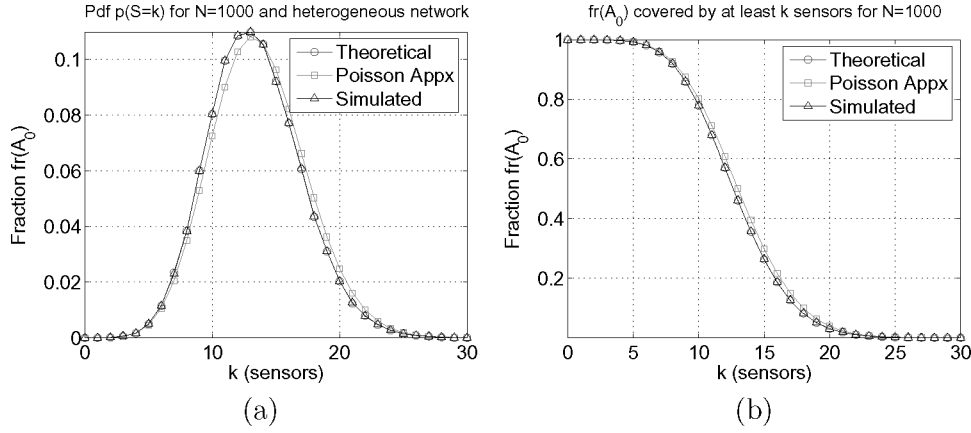


Fig. 11. Heterogeneous sensor network, with FoI being a disk of radius $R = 100$ m. An equal number of two types of sensors are deployed; Type A has a sensing area of a disk shape with radius $r_A = 10$ m, while type B has a sensing area of a disk shape with $r_B = 15$ m. (a) The pdf of the fraction $fr(\mathcal{A}_0)$ covered by exactly k sensors when $N = 1000$ sensors. (b) The fraction $fr(\mathcal{A}_0)$ covered by at least k sensors when $N = 1000$ sensors.

increase of N . This is due to the fact that as the number of deployed sensors increases, more sensors will be deployed at the border of the deployment region and, hence, the border effect becomes more significant. On the other hand no such pattern occurs for the KL-distance between our theoretical result and the simulations.

In Figure 10(b), we show the fraction of \mathcal{A}_0 covered by *at least* k sensors when $N = 300$. The same graphs for $N = 500$, $N = 1000$ are provided in Figures 10(d) and 11(b), respectively. For all graphs in Figures 6 and 7, we show the theoretical result according to our expressions and the simulation values, as well as the Poisson approximation.

In the case of heterogeneous sensor networks where each sensor has a different sensing area, the formula in (43) has an exponentially increasing computational cost, since an exponentially increasing summation of terms must be computed in order to derive the exact coverage achieved. Such a computation may not be feasible for large networks. The higher accuracy obtained using the exact formula does not justify the tradeoff in computational complexity with respect to the Poisson approximation provided by Miorandi and Altman [2005].

In such a case, a similar approximation can be used for our formulas by employing the expressions derived for a homogeneous sensor network and substituting the size F and perimeter L of the sensing area of the sensors with the expected size $E[F]$ and expected perimeter $E[L]$. The theoretical approximation for such a case is

$$fr(\mathcal{A}_0) = p(S = k) = \frac{\binom{N}{k} (2\pi E[F])^k (2\pi F_0 + L_0 E[L])^{N-k}}{(2\pi (F_0 + E[F]) + L_0 E[L])^N}. \quad (45)$$

In Figure 12(a), we show the pdf obtained via simulation for our heterogeneous sensor network experiment, for $N = 500$ sensors, the theoretical values based on the exact formula in (43), the Poisson approximation in (44), and the

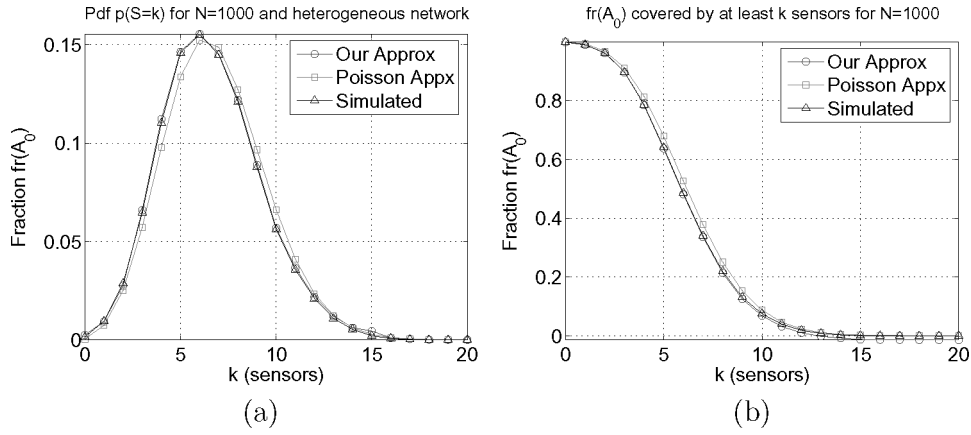


Fig. 12. Heterogeneous sensor network, with FoI being a disk of radius $R = 100$ m. An equal number of two types of sensors are deployed; Type A has a sensing area of a disk shape with radius $r_A = 10$ m, while type B has a sensing area of a disk shape with radius $r_B = 15$ m. (a) The pdf of the fraction $fr(\mathcal{A}_0)$ covered by exactly k sensors when $N = 500$ sensors. (b) The fraction $fr(\mathcal{A}_0)$ covered by at least k sensors when $N = 500$ sensors.

approximation in (45). In Figure 12(b), we show the fraction of \mathcal{A}_0 covered by at least k sensors. We observe that, for the case of heterogeneous sensor networks where each sensor has a different sensing area, (45) provides a better approximation than the (44), without incurring the computational cost of (43). The KL-distance for the approximation obtained via (45) is equal to 2.3×10^{-3} , while the Poisson approximation gives a KL-distance equal to 6.8×10^{-3} . With respect to the worst case, the TV-distance for the approximation obtained via (45) is equal to 6.4×10^{-3} , while the Poisson approximation gives a TV-distance equal to 54.6×10^{-3} .

5.4 An Example of Computing the Coverage in a Sample Network

In this section, we provide an example of applying our results to a sample sensor network. Consider an FoI of size $F_0 = 10^6 \text{ m}^2$ and perimeter $L_0 = 4,000$ m where sensors of identical sensing area $F = 100\pi$ and perimeter $L = 20\pi$ are randomly deployed. We want to compute the number of sensors needed in order for a randomly selected point of the FoI to be covered by at least one sensor with a probability $p_C = 95\%$. Or alternatively, the number of sensors N needed, so that a fraction $p_C = 0.95$ of the field of interest is covered by at least one sensor.

Lemma 4.6 and Corollary 4.8 yield

$$\begin{aligned}
 p(S \geq 1) &= 1 - p(S = 0) \\
 &= 1 - \prod_{i=1}^N \left(\frac{2\pi F_0 + L_0 L}{2\pi(F_0 + F) + L_0 L} \right) \\
 &= 1 - \left(\frac{2\pi F_0 + L_0 L}{2\pi(F_0 + F) + L_0 L} \right)^N.
 \end{aligned}$$

We want the probability of 1-coverage to be at least $p(S \geq 1) \geq p$. Hence,

$$P(S \geq 1) = 1 - \left(\frac{2\pi F_0 + L_0 L}{2\pi(F_0 + F) + L_0 L} \right)^N \geq p_C \Rightarrow$$

$$N \geq \frac{\log(1 - p_C)}{\log\left(\frac{2\pi F_0 + L_0 L}{2\pi(F_0 + F) + L_0 L}\right)}.$$

Substituting the values for p_C, F_0, L_0, F, L yields $N \geq 9728$ sensors.

6. CONCLUSION

We studied the problem of stochastic coverage in heterogeneous sensor networks. By mapping the coverage problem to the set intersection problem, we derived analytical formulas that compute the k -coverage when sensors are deployed in a field of interest according to an arbitrary distribution Y . In our analysis, the sensors can have a sensing area of any shape and also need not have identical sensing areas. We provided simplified expressions for the case when the sensors are randomly deployed, as well as when the sensors have identical sensing areas.

We verified our theoretical results via simulation and compared them with previous formulas that characterized coverage in both homogeneous and heterogeneous sensor networks. By evaluating the KL-distance between the analytic coverage formulas and the simulation, we showed that our expressions provide a significantly higher accuracy. This is due to the fact that our results do not suffer from the border effects and hold exactly rather than approximately. We also provided examples on how to utilize our expressions in order to compute the number of sensors that need to be deployed in a field of interest, so that a coverage requirement is met.

APPENDIX: A. MEASURE OF ALL MOTIONS OF \mathcal{A}_1 SUCH THAT IT INTERSECTS WITH \mathcal{A}_0

In this section, we compute the measure of all motions of \mathcal{A}_1 such that $\mathcal{A}_0 \cap \mathcal{A}_1 \neq \emptyset$:

$$\begin{aligned} m(\mathcal{A}_1 : \mathcal{A}_0 \cap \mathcal{A}_1 \neq \emptyset) &\stackrel{\text{(i)}}{=} \int_{\mathcal{A}_0 \cap \mathcal{A}_1 \neq \emptyset} d\mathcal{A}_1 \\ &\stackrel{\text{(ii)}}{=} \int_{\mathcal{A}_0 \cap \mathcal{A}_1 \neq \emptyset} dx \wedge dy \wedge d\phi \\ &\stackrel{\text{(iii)}}{=} \int_0^{2\pi} (F_0 + F_1 + 2F_{01}) d\phi \\ &\stackrel{\text{(iv)}}{=} 2\pi(F_0 + F_1) + L_0 L_1. \end{aligned} \tag{46}$$

In (i), we integrate the kinematic density $d\mathcal{A}_1$ of set \mathcal{A}_1 over all motions of \mathcal{A}_1 such that $\mathcal{A}_0 \cap \mathcal{A}_1 \neq \emptyset$. In (ii), we write the kinematic density in its expanded differential form as defined in (2). In (iii), we compute the area between

$\mathcal{A}_0, \mathcal{A}_1$, which is called *mixed area of Minkowski*, and integrate over all possible rotations. The integration yields the desired result.

A.1 Proof of (iii)

The proof is due to Santalo [1936, 1976]. Let $\mathcal{A}_0, \mathcal{A}_1$ be two convex sets with support functions $p_0(\phi), p_1(\phi)$, respectively. The support function $p(\phi)$ of a convex set \mathcal{A} denotes the distance of the origin point of a convex set from the envelope that defines the curve that bounds the convex set, as a function of the angle ϕ of the envelope with the x -axis of the coordinate system. Let $\mathcal{A}_0, \mathcal{A}_1$ intersect and let \mathcal{A}_{01} denote the common area between $\mathcal{A}_0, \mathcal{A}_1$. \mathcal{A}_{01} is called the *mixed convex set* of $\mathcal{A}_0, \mathcal{A}_1$, and has a support function $p(\phi) = p_0(\phi) + p_1(\phi)$.

The area of the mixed convex set can be computed by the decomposition into elementary triangles of height equal to p and base equal to ds , where ds is the elementary arc of the convex curve that bounds \mathcal{A}_{01} :

$$\begin{aligned}
 F &= \frac{1}{2} \int_{d\mathcal{A}_{01}} p ds \\
 &\stackrel{(i)}{=} \frac{1}{2} \int_0^{2\pi} p(p + p') d\phi \\
 &\stackrel{(ii)}{=} \frac{1}{2} \int_0^{2\pi} (p^2 - p'^2) d\phi \\
 &\stackrel{(iii)}{=} \frac{1}{2} \int_0^{2\pi} ((p_0 + p_1)^2 - (p_0' + p_1')^2) d\phi \\
 &= \frac{1}{2} \int_0^{2\pi} (p_0^2 - p_0'^2) d\phi + \frac{1}{2} \int_0^{2\pi} (p_1^2 - p_1'^2) d\phi + \frac{1}{2} \int_0^{2\pi} (p_0 p_1 - p_0' p_1') d\phi \\
 &= F_0 + F_1 + 2F_{01}, \tag{47}
 \end{aligned}$$

where

$$F_{01} = \frac{1}{2} \int_0^{2\pi} (p_0 p_1 - p_0' p_1'). \tag{48}$$

Equation (i), is due by the definition of the support function [Bonnesen and Fenchel 1934; Santalo 1976]. In (ii) we do integration by parts, and in (iii) we replace $p = p_0 + p_1$.

A.2 Proof of (iv)

In this section, we want to compute the integral

$$I = \int_0^{2\pi} (F_0 + F_1 + 2F_{01}) d\phi. \tag{49}$$

The computation is as follows:

$$\begin{aligned}
 I &= \int_0^{2\pi} (F_0 + F_1 + 2F_{01}) d\phi \\
 &= 2\pi F_0 + 2\pi F_1 + \int_0^{2\pi} 2F_{01} d\phi. \tag{50}
 \end{aligned}$$

$$\begin{aligned}
 F_{01} &= \frac{1}{2} \int_0^{2\pi} (p_0 p_1 - p'_0 p'_1) d\phi \\
 &\stackrel{\text{(i)}}{=} \frac{1}{2} \int_0^{2\pi} (p_0(p_1 + p'_1)) d\phi \\
 &\stackrel{\text{(ii)}}{=} \frac{1}{2} \int_{dA_1} p_0 ds_1 \\
 &\stackrel{\text{(iii)}}{=} \frac{1}{2} \int_{dA_1} p_0(\phi - \theta) ds_1.
 \end{aligned} \tag{51}$$

Equation (i) is obtained by performing integration by parts. In (ii), we replace $p_1 + p'_1$, with ds_1 ([Bonnesen and Fenchel 1934; Santalo 1976]). In (iii), we consider all possible rotations θ of A_1 , such that A_1 intersects with A_0 . Integrating over all θ yields

$$\begin{aligned}
 \int_0^{2\pi} F_{01}(\theta) d\theta &= \int_0^{2\pi} \left(\frac{1}{2} \int_{dA_1} p_0(\phi - \theta) ds_1 \right) d\theta \\
 &= \frac{1}{2} \int_{dA_1} \left(\int_0^{2\pi} p_0(\phi - \theta) d\theta \right) ds_1 \\
 &= \frac{1}{2} \int_{dA_1} L_0 ds_1 \\
 &= \frac{1}{2} L_0 L_1,
 \end{aligned} \tag{52}$$

where we have used the fact that [Santalo 1976]

$$\int_0^{2\pi} p_0 d\theta = L_0, \quad \int_{dA_1} ds_1 = L_1. \tag{53}$$

Substituting (52) into (50) yields

$$I = 2\pi F_0 + 2\pi F_1 + L_0 L_1. \tag{54}$$

REFERENCES

- AKYILDIZ, I., SU, W., SANKARASUBRAMANIAM, Y., AND CAYIRCI, E. 2002. A survey on sensor networks. *IEEE Commun. Mag.* 40, 8, 102–114.
- BETTSTETTER, C. AND KRAUSE, O. 2001. On border effects in modeling and simulation of wireless ad hoc networks. In *Proceedings of the IEEE MWCN '01*.
- BETTSTETTER, C. AND ZANGL, J. 2002. How to achieve a connected ad hoc network with homogeneous range assignment: An analytical study with consideration of border effects. In *Proceedings of the WCNC '02*. 125–129.
- BLASCHKE, W. 1955. *Vorlesungen über Integralgeometrie 9*, 3rd Ed. Deutscher Verlag Wiss, Berlin, Germany.
- BONNESEN, T. AND FENCHEL, W. 1934. Theorie der convexen Körper. *Ergeb. Math.* Springer, Berlin, Germany, 18.
- COVER, T. M. AND THOMAS, A. 1991. *Elements of Information Theory*. John Wiley and Sons, New York, NY.
- FILIPESCU, D. 1971. On some integral formulas relative to convex figures in the euclidean space e_2 . *Stud. Cerc. Mat.* 23, 693–709.

- FLANDERS, H. 1963. *Differential Forms with Applications to the Physical Sciences*. Academic Press, New York, NY.
- FLANDERS, H. 1967. *Differential Forms*. Prentice Hall, Englewood Cliffs, NJ.
- GUPTA, H., DAS, S. R., AND GU, Q. 2003. Connected sensor cover: Self-organization of sensor networks for efficient query execution. In *Proceedings of the 4th ACM International Symposium on Mobile Ad Hoc Networking & Computing (MobiHoc '03)*. 189–200.
- KAR, K. AND BANERJEE, S. 2003. Node placement for connected coverage in sensor networks. In *Proceedings of WiOpt '03*.
- KOUSHANFAR, F., MEGUERDICHIAN, S., POTKONJAK, M., AND SRIVASTAVA, M. 2001. Coverage problems in wireless ad-hoc sensor networks. In *Proceedings of IEEE INFOCOM '01*. 1380–1387.
- KRISHNAMACHARI, B., ESTRIN, D., AND WICKER, S. B. 2002. The impact of data aggregation in wireless sensor networks. In *Proceedings of the 22nd International Conference on Distributed Computing Systems (ICDCSW '02)*. 575–578.
- LI, X., WAN, P., AND FRIEDER, O. 2003. Coverage in wireless ad hoc sensor networks. *IEEE Trans. Comput.* 52, 6, 753–763.
- LIU, B. AND TOWSLEY, D. 2004. A study of the coverage of large-scale sensor networks. In *Proceedings of MASS '04*.
- MAINWARING, A., POLASTRE, J., SZEWCZYK, R., CULLER, D., AND ANDERSON, J. 2002. Wireless sensor networks for habitat monitoring. In *Proceedings of the 1st ACM International Workshop Wireless Sensor Networks and Applications*.
- MEGUERDICHIAN, S., KOUSHANFAR, F., QU, G., AND POTKONJAK, M. 2001. Exposure in wireless ad hoc sensor networks. In *Proceedings of MobiCom '01*. 139–150.
- MILES, R. 1969. The asymptotic values of certain coverage probabilities. *Biometrika* 56, 661–680.
- MIORANDI, D. AND ALTMAN, E. 2005. Coverage and connectivity of ad hoc networks in presence of channel randomness. In *Proceedings of IEEE INFOCOM '05*. 491–502.
- PODURI, S. AND SUKHATME, G. S. 2004. Constrained coverage for mobile sensor networks. In *Proceedings of the IEEE International Conference on Robotics and Automation '04*. 165–172.
- SANTALO, L. 1936. Geometrica integrale 4: Sobre la medida cinematica en el plano. *Abh. Math. Sem. Univ. Hamburg* 11, 222–236.
- SANTALO, L. 1976. *Integral Geometry and Geometric Probability*. Addison-Wesley, Reading, MA.
- STOKA, M. 1969. Alcune formule integrali concernenti i corpi convessi dello spazio euclideo e_3 . *Rend. Sem. Mat. Torino* 28, 95–108.
- SZEWCZYK, R., OSTERWEIL, E., POLASTRE, J., HAMILTON, M., MAINWARING, A., AND ESTRIN, D. 2004. Habitat monitoring with sensor networks. *Commun. ACM* 47, 6, 34–40.
- XING, G., WANG, X., ZHANG, Y., LU, C., PLESS, R., AND GILL, C. 2005. Integrated coverage and connectivity configuration for energy conservation in sensor networks. *Trans. Sensor Netw.* 1, 1, 36–72.

Received December 2005; revised June 2006; accepted June 2006